

# Institutionen för systemteknik

## Department of Electrical Engineering

Examensarbete

### Development and Evaluation of Model-Based Misfire Detection Algorithm

Examensarbete utfört i Fordonssystem  
vid Tekniska högskolan vid Linköpings universitet  
av

**Linus Therén**

LiTH-ISY-EX--14/4807--SE

Linköping 2014



**Linköpings universitet**  
**TEKNISKA HÖGSKOLAN**



# Development and Evaluation of Model-Based Misfire Detection Algorithm

Examensarbete utfört i Fordonssystem  
vid Tekniska högskolan vid Linköpings universitet  
av

**Linus Therén**

LiTH-ISY-EX--14/4807--SE

Handledare: **Daniel Jung**  
ISY, Linköpings Universitet  
**Per Ericson**  
Volvo Cars Corporation

Examinator: **Erik Frisk**  
ISY, Linköpings Universitet

Linköping, 14 november 2014



	<b>Avdelning, Institution</b> Division, Department	<b>Datum</b> Date
	Division of Vehicular Systems Department of Electrical Engineering SE-581 83 Linköping	2014-11-14

<b>Språk</b> Language <input type="checkbox"/> Svenska/Swedish <input checked="" type="checkbox"/> Engelska/English <input type="checkbox"/> _____	<b>Rapporttyp</b> Report category <input type="checkbox"/> Licentiatavhandling <input checked="" type="checkbox"/> Examensarbete <input type="checkbox"/> C-uppsats <input type="checkbox"/> D-uppsats <input type="checkbox"/> Övrig rapport <input type="checkbox"/> _____	<b>ISBN</b> _____ <b>ISRN</b> LiTH-ISY-EX--14/4807--SE <b>Serietitel och serienummer</b> <b>ISSN</b> Title of series, numbering                      _____
--	---	---

**URL för elektronisk version**

<http://urn.kb.se/resolve?urn=urn:nbn:se:liu:diva-XXXXX>

<b>Titel</b> Title	Utveckling och Utvärdering av Algoritm för Modellbaserad Misständningsdetektion Development and Evaluation of Model-Based Misfire Detection Algorithm
<b>Författare</b> Author	Linus Therén

**Sammanfattning**  
 Abstract

This report present the work to develop a misfire detection algorithm for on-board diagnostics on a spark ignited combustion engine. The work is based on a previous developed model-based detection algorithm, created to meet more stringent future legislation and reduce the cost of calibration. In the existing approach a simplified engine model is used to estimate the torque from the flywheel angular velocity, and the algorithm can detect misfires in various conditions.

The main contribution in this work, is further development of the misfire detection algorithm with focus on improving the handling of disturbances and variations between different vehicles. The resulting detection algorithm can be automatically calibrated with training data and manage disturbances such as manufacturing errors on the flywheel and torsional vibrations in the crankshaft occurring after a misfire. Furthermore a robustness analysis with different engine configurations is carried out, and the algorithm is evaluated with the Kullback-Leibler divergence correlated to the diagnosis requirements. In the validation, data from vehicles with four cylinder engines are used and the algorithm show good performance with few false alarms and missed detections.

<b>Nyckelord</b> Keywords	Model-Based, Misfire, Detection , Diagnosis, Kullback-Leibler, SVM
------------------------------	--



## **Abstract**

This report presents the work to develop a misfire detection algorithm for on-board diagnostics on a spark ignited combustion engine. The work is based on a previously developed model-based detection algorithm, created to meet more stringent future legislation and reduce the cost of calibration. In the existing approach a simplified engine model is used to estimate the torque from the flywheel angular velocity, and the algorithm can detect misfires in various conditions.

The main contribution in this work, is further development of the misfire detection algorithm with focus on improving the handling of disturbances and variations between different vehicles. The resulting detection algorithm can be automatically calibrated with training data and manage disturbances such as manufacturing errors on the flywheel and torsional vibrations in the crankshaft occurring after a misfire. Furthermore a robustness analysis with different engine configurations is carried out, and the algorithm is evaluated with the Kullback-Leibler divergence correlated to the diagnosis requirements.

In the validation, data from vehicles with four cylinder engines are used and the algorithm shows good performance with few false alarms and missed detections.



## Sammanfattning

I denna rapport presenteras arbetet med utveckling av en algoritm för misstänningsdetektion lämplig för fordonsbunden övervakning i gnisttända förbränningsmotorer. Arbetet baseras på ett tidigare utvecklad modellbaserad algoritm, skapad för att klara framtida strängare krav samt för att minska kalibreringsbördan. I den befintliga metoden används en enklare motormodell för att skatta momentet från svänghjulets vinkelhastighet och algoritmen kan upptäcka misständningar i varierande förhållanden.

Det största bidraget i arbetet är vidareutvecklingen av detektionsalgoritmen med fokus på förbättrad hantering av störningar och variationer mellan fordon. Den resulterande detektionsalgoritmen kan automatiskt kalibreras med träningsdata och hanterar störningar som tillverkningsfel på svänghjulet och vibrationer i vevaxeln efter en misständning. Vidare görs en analys av robustheten med olika motorkonfigurationer, och algoritmen utvärderas med Kullback-Leibler divergensten i korrelation med kraven satta på diagnosen.

I valideringen, används data från fordon med fyrcylindriga motorer och algoritmen visar god prestanda med få falsklarm och missade detektioner.



## **Acknowledgments**

First of all I would like thank my supervisor Daniel Jung at Linköpings University for all his help and feedback as well as letting me base my work on his research. Secondly I wish to thank Per Ericson and Sasa Trajkovic at Volvo Cars for the help and guidance. Also a special thanks to Volvo Cars for giving me the opportunity to write this thesis.

Finally I want to thank my family for all the support and encouragement.

*Värnamo, September 2014  
Linus Therén*



---

# Contents

<b>1</b>	<b>Introduction</b>	<b>1</b>
1.1	Background . . . . .	1
1.2	Goals and purpose . . . . .	3
1.3	Method . . . . .	3
1.4	Related research . . . . .	4
<b>2</b>	<b>Data and signals</b>	<b>7</b>
2.1	Data . . . . .	7
2.2	Signals . . . . .	8
2.2.1	Flywheel angular velocity . . . . .	8
2.2.2	Air mass flow . . . . .	8
2.2.3	Catalyst warming flag . . . . .	9
2.2.4	Crank angle counter and sampling . . . . .	9
<b>3</b>	<b>Engine torque model</b>	<b>11</b>
3.1	Torque estimation . . . . .	11
3.2	Distinguishing misfire from nominal behavior . . . . .	13
3.2.1	Pre-processing of the estimated torque . . . . .	14
3.3	Cold starts . . . . .	16
<b>4</b>	<b>Misfire detection algorithm</b>	<b>17</b>
4.1	Operating points . . . . .	17
4.2	Hypothesis test . . . . .	18
4.3	Design of test quantity . . . . .	18
4.4	Parameterization . . . . .	19
4.5	Summary . . . . .	20
<b>5</b>	<b>Kullback-Leibler divergence correlated to Volvo KPI</b>	<b>21</b>
5.1	Kullback-Leibler divergence . . . . .	21
5.2	Volvo KPI . . . . .	22
5.3	Correlation . . . . .	23
5.4	Conclusion . . . . .	25

---

<b>6</b>	<b>Robustness analysis of misfire detection algorithm</b>	<b>27</b>
6.1	Varying number of cylinders . . . . .	27
6.1.1	Misfire Visibility . . . . .	28
6.1.2	Misfire detectability performance . . . . .	31
6.2	Vehicle to vehicle variations . . . . .	32
6.2.1	Pitch error modeling . . . . .	32
6.2.2	Compensation . . . . .	34
6.3	Torsional vibrations in the crankshaft . . . . .	36
6.3.1	Model . . . . .	36
6.3.2	Compensation . . . . .	37
<b>7</b>	<b>Evaluation</b>	<b>41</b>
7.1	Training and validation data . . . . .	41
7.2	Evaluation of misfire detection algorithm . . . . .	42
7.3	Compensation for vehicle to vehicle variations . . . . .	45
7.4	Compensation for torsional vibrations . . . . .	47
7.5	Summary and discussion . . . . .	51
<b>8</b>	<b>Conclusions and future work</b>	<b>53</b>
8.1	Conclusions . . . . .	53
8.2	Future work . . . . .	54
	<b>Bibliography</b>	<b>57</b>

# 1

---

## Introduction

The thesis is written at Volvo Cars in Gothenburg and focuses on misfire detection in internal combustion engines. This introducing chapter contains the background and description of the problem as well as the goals and purpose of the thesis.

### 1.1 Background

Monitoring of automotive engines is becoming more important as the requirements of reliability and environmental friendliness increases. The on-board diagnostics (OBDII) legislations were introduced in 1994, which require that vehicle emissions and its underlying factors must be monitored on-board the vehicle [1]. One of the OBDII requirements is that engine misfires must be detected.

Engine misfires is a phenomenon that describe incomplete combustions in the engine cylinders. A misfire will induce a raised level of exhaust emissions and may also damage the catalytic converter, which strongly influence the performance of the automotive exhaust emission control system, see [18].

Detecting engine misfire is a non-trivial task complicated by several factors such as vibrations, manufacturing errors, cold starts, and varying speeds and loads, see [7]. The problem is further complicated by the fact that the on-board computational power in a vehicle is limited, and therefore the implemented detection algorithm needs to be held at a low complexity.

In conjunction with the introduction of a new engine generation with four cylinder engines, Volvo is investigating in new algorithms that have good detection performance but at the same time are easy to calibrate. As the demands of rapidly

launching new vehicle models to attract customers, an alternative method that reduces the manual calibration effort is pursued.

When an engine misfire occurs, it results in a reduced rise of the cylinder pressure as a result of the incomplete combustion. Since the use of an in cylinder pressure gauge is considered to be both too expensive and have poor durability [13], it is not used in mass produced automobiles. Instead a transient decrease in the rotational speed of the crankshaft is utilized to detect a misfire. An example of how a misfire appear in the rotational speed of the crankshaft is shown in Figure 1.1, where the misfire is injected around sample 100.

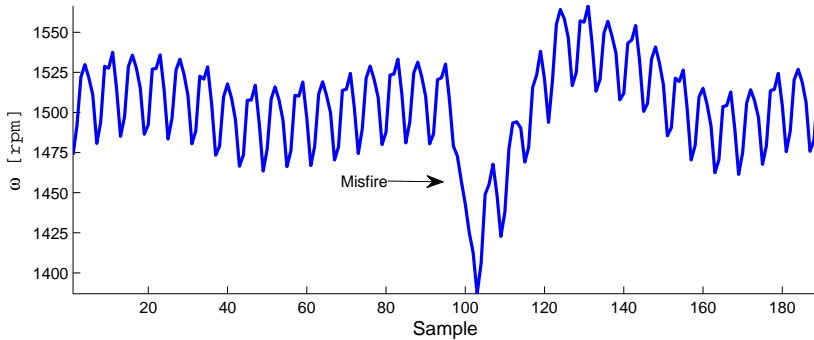


**Figure 1.1:** Flywheel angular velocity measurements around speed 1500rpm and load 0.8g/rev with an injected misfire around sample 100.

The basis of this thesis is a model-based misfire detection algorithm that has been developed in collaboration between Linköpings University and Volvo Cars, see [12]. The introduction of a new generation of Volvo engines with four cylinders instead of previous generations with five and six cylinders require that the detection algorithm is adjusted and additional investigations are required to ensure that the method is robust. Although the developed misfire detection algorithm can handle the majority of the mentioned complications such as varying engine speed and load, potential improvements can be made in the area of disturbance handling. Torsional vibrations in the crankshaft after a misfire are pointed out as a problem in [12], since it causes oscillations in the signal and thus increase the risk of false alarms. Other potential sources of errors in a model-based misfire detection approach are vehicle to vehicle variations such as manufacturing errors, wear out, and deviating frictions. These mentioned potential vehicle to vehicle errors causes systematic distortions and thus need to be investigated and compensated for to improve the detectability performance.

To evaluate the detectability of misfires and quantify the performance of the misfire detection algorithm the Kullback-Leibler divergence is proposed [12]. The interpretation of the Kullback-Leibler divergence is intuitive for comparative purposes, but the relation to Volvo KPI (Key Performance Indicator), which are the requirements on the misfire detection algorithm used by Volvo, are not fully eval-

uated. Volvo KPI include legal requirements regarding detection of misfires, and internal requirements at Volvo to avoid false alarms and thereby prevent unnecessary warranty expenses.

## 1.2 Goals and purpose

The purpose of this master thesis is to investigate and further develop the model-based misfire detection algorithm proposed in [12] in the means of detectability and disturbance handling. Another goal is to investigate the use of the Kullback-Leibler divergence as an misfire detection performance evaluation tool and relate the result to Volvo's requirements. The goal can be divided in the following bullets:

- Adapt the misfire detection algorithm in [12] for four-cylinder engines and evaluate the misfire detection performance. The result is compared to the detection performance in six-cylinder engines.
- Investigate the impact of vehicle to vehicle variations and how to compensate for such variations in the detection algorithm.
- Investigate how to compensate in the algorithm for vibrations in the powertrain following a misfire.
- Investigate the Kullback-Leibler divergence in terms of misfire detection performance, and how it relates to the requirements set by Volvo.

## 1.3 Method

In model-based diagnosis system design, the principle is to develop a model that describe the fault-free behavior while the effects of the different faults is known, see for example [8]. In the case of misfire diagnosis two behavioral modes is considered: fault-free combustion and misfire.

$NF$  no fault

$F_{mf}$  misfire

Thus the purpose of the detection algorithm is to create a test quantity for the hypothesis test such that when a misfire occurs the null hypothesis is rejected

$$H^0 : F_p \in NF$$

$$H^1 : F_p \in F_{mf}$$

where  $F_p$  is the present behavioral mode.

In [8], a systematic design procedure for such diagnosis systems is suggested which this work mainly follows. The steps can be summarized as:

1. Define which faults that are diagnosed and what the requirements are.
2. Study the system and the faults that are diagnosed.
3. Build a model of the process in the fault-free case.
4. Investigate how the fault influence the system.
5. Design a test quantity to be used in the hypothesis tests.
6. Evaluate the diagnosis system in simulations and if possible in reality. If the performance is not satisfactory, refine the model or the test.
7. Final implementation of the diagnosis system.

In this thesis, no final implementation is made. However, steps 1-6 in the procedure are considered in the design process and the evaluation is done with measurements both from test rig and on road.

## 1.4 Related research

Misfire detection is a well-covered area in the literature and many various methods are proposed. In [16], a survey is presented of research regarding diagnosis algorithms for automotive applications, for example misfire detection methods. A proven strategy for misfire detection is to measure the time between the predetermined angular interval on the flywheel to estimate its angular velocity, see [18]. The flywheel angular velocity of the flywheel can then be filtered using signal processing to classify misfires, see [7]. Such methods based on the angular velocity often performs well at low speed, but experience difficulties at higher engine speeds due to increasing vibrations according to [16]. Another common strategy is the use of the angular velocity signal to estimate engine torque in a model-based approach, see for example [12, 13, 18]. One of the difficulties in a model-based approach lies in succeeding to balance between keeping low complexity in order to enable on-board detection, and process errors and imperfections to get a high detectability. In [13], a Kalman filter approach is presented using a simplified engine model that also features compensation for disturbances. However the algorithm experience difficulties at higher speeds due to reduced signal-to-noise ratio. Another method is used in [18] where torque waveforms nonuniformity is utilized to detect misfiring cylinders where [18] also argues for the use of the frequency domain to detect misfires.

An analytical model for the cylinder pressure is developed in [6] where the method is based on a parameterization of the ideal Otto cycle. The in-cylinder pressure is given as a function of crank angle, manifold pressure, manifold temperature and spark timing and requires fine tuning but could then be used in on-line applications.

---

The work in this master thesis is based on and a continuation of the work in [12]. A model-based approach is proposed where the indicated torque is estimated from the angular velocity signal and an algorithm is developed that is kept at low complexity to enable on-line misfire detection. Furthermore, [12] addresses the idea to use the Kullback-Leibler divergence for quantitative fault detection analysis. The Kullback-Leibler divergence is a widely used tool in statistics and pattern recognition to evaluate the similarity between two distributions. However, in [12] it is suggested to evaluate the dissimilarity between fault-free data and misfire data. The advantages of using the Kullback-Leibler distance between distributions is discussed in [14] where the Kullback-Leibler distance is highlighted as conceptually simpler than the use of probability.



# 2

---

## Data and signals

This chapter briefly describes how data is collected and which data that is used in this work. Also the signals used during the design process are presented.

### 2.1 Data

The data used in this work are collected from five Volvo cars with four and six cylinder engines. The measurements are either collected in a chassis dynamometer or during real driving scenarios on the road. In all data sets, misfires are injected periodically in all cylinders one at the time, always with several engine cycles in between. The measurements from the chassis dynamometer are collected

Data set	Vehicle	Num.Cyl.	Condition	Num.Comb.
1	1	4	FTP75	70794
2	1	4	FTP75	69053
3	1	4	FTP75	74641
4	2	4	On the road	31995
5	3	4	Steady state	573202
6	4	4	Steady state	92232
7	2	4	Steady state	540083
8	5	6	Steady state	688884

**Table 2.1:** Data used to train and evaluate the misfire detection algorithm. *Num.Comb* is an abbreviation for the number of combustions included in the measurement and *Num.Cyl* is the number of cylinders in the engine.

indoors without disturbances from environmental conditions, such as varying driving surfaces and whether conditions, which make them suitable for comparisons. Such measurements are available both from steady state conditions with constant speed and load or following the FTP75 driving cycle. The FTP75 cycle is a city driving scenario that includes cold starts but is limited to lower engine speeds. Data set 4 is a real driving scenario with measurement on the road that includes higher engine speed but no cold starts. Data sets 5, 6, 7, and 8 contains steady state measurements covering several engine operating points including cold starts. In Table 2.1 the measurement condition and vehicle for each data set are shown.

## 2.2 Signals

Four signals shown in Table 2.2, from the vehicle's control system are used by the algorithm in this work to monitor all driving cases. The function and purpose of each signal are briefly described below.

Signal	Variable	Unit
Flywheel angular velocity	$\omega$	rpm
Air mass flow	$m_a$	g/rev
Catalyst warming flag	–	–
Crank angle counter	–	–

*Table 2.2: List of the used signals in the algorithm.*

### 2.2.1 Flywheel angular velocity

The angular velocity is the prime signal used in detection of misfires. When a misfire occur, it introduces an instantaneous reduction in the angular velocity and it is this reduction that is utilized to detect misfires. The angular velocity is also used to categorize the engine behaviour in different operating points based on speed.

The angular velocity is not directly measured, but calculated from the original signal that count the time between two succeeding teeth on the flywheel with a high frequency clock [18]. One sample of the angular velocity can then be obtained by the equation

$$\omega_i = \frac{\theta_i - \theta_{i-1}}{\Delta t_i} \quad (2.1)$$

where  $\Delta t_i$  is the segment time for the fixed angular interval  $\theta_i - \theta_{i-1}$ . An example of the appearance of the flywheel angular velocity signal is shown in Figure 2.1.

### 2.2.2 Air mass flow

The appearance of the flywheel angular velocity signal depend on several various causes. The engine load is one such factor and together with the engine speed, it is often used to categorize the engine behaviour in different operating points [7].

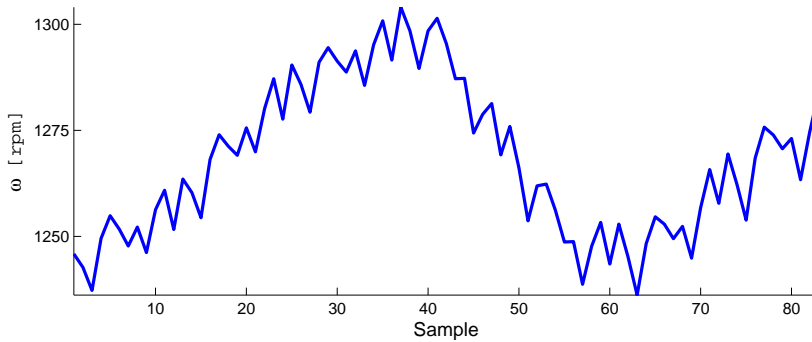


**Figure 2.1:** Flywheel angular velocity signal around 1275 rpm and load 0.3 g/rev.

In [12], a used approximation is that the air mass flow varies proportionally to the intake manifold pressure. Thereby the air mass flow can be used to represent the engine load. The same approximation is used in this work.

### 2.2.3 Catalyst warming flag

The catalyst warming flag is set to point out that the catalytic converter is cold. When the catalytic converter is cold it needs to be heated up to function properly and thus avoid unnecessary exhaust. This is typically done by increasing amount of fuel and delaying the ignition of the fuel mixture in order to heat up the exhaust gas. This combined with an overall cold engine gives an engine behavior that deviates from the behaviour in normal conditions and complicates misfire detection.

### 2.2.4 Crank angle counter and sampling

The crank angle counter contains the position on the flywheel of each sample and depends on the sampling resolution of the angular velocity. Current flywheel standards allow sampling of every  $6^\circ$  on the flywheel [13]. Although, such a high resolution contains more information about the combustions, it requires more computational power and also introduce more quantization noise and uncertainties due to the manufacturing imperfections.

In this work, the angular resolution is set to  $30^\circ$ , which means that a full engine cycle, i.e. two revolutions, result in  $2 \cdot 360^\circ / 30^\circ = 24$  samples. These samples are represented by crank counts 1, 2, ..., 24 where crank count 1 represent an interval starting approximately  $20^\circ$  before top dead center of cylinder 1.

The crank counts are assigned to each cylinder such that the interval from the ignition of the cylinder until the ignition of the next cylinder is covered. The misfiring cylinder can thereby be identified through the crank counts, as the effects of a misfire are isolated to an interval in the signal. Thus in a four cylinder engine, six crank counts are paired with each cylinder while four samples are paired with

each cylinder in a six cylinder engine. The firing order of the cylinders is 1-3-4-2 in the four cylinder engine and 1-5-3-6-2-4 in the six cylinder engine, which give the association of crank counts to each cylinder that are presented in Table 2.3. During cold start, the crank counts are assigned with one step offset in the six cylinder engine, as the ignition is delayed [12]. This is not necessary in four cylinder engines as the combustion are more separated and the effects of a misfire are still within the assigned interval.

An example of computed angular velocity  $\omega$  from a four cylinder vehicle during one cycle and corresponding crank counts is presented in Figure 2.2. In the figure, the assigned crank count intervals in Table 2.3 clearly include the increase in angular velocity connected to each cylinder combustion.

Cylinder	Crank count	
	4-cyl.engine	6-cyl.engine
1	1, 2, 3, 4, 5, 6	1, 2, 3, 4
2	19, 20, 21, 22, 23, 24	17, 18, 19, 20
3	7, 8, 9, 10, 11, 12	9, 10, 11, 12
4	13, 14, 15, 16, 17, 18	21, 22, 23, 24
5		5, 6, 7, 8
6		13, 14, 15, 16

**Table 2.3:** The crank counts that are associated to each cylinder.

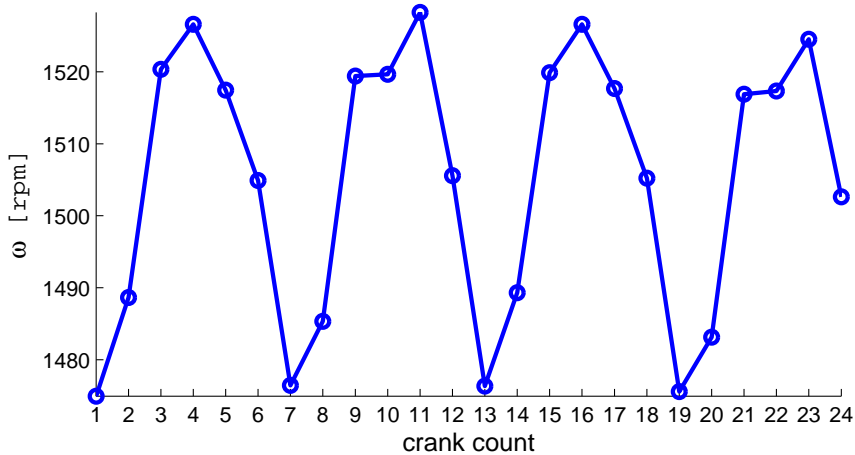


**Figure 2.2:** Flywheel angular velocity at 1500rpm and load 0.8g/rev and the corresponding crank counts.

# 3

---

## Engine torque model

In this chapter the engine torque model described in [12] is presented and the connection to the previous presented flywheel signal is shown. The model output is an estimate of the torque at the crankshaft, which is further processed according to [12] in order to enhance the effect of a misfire. The result is discussed and the visibility of a misfire is analyzed for various conditions and operating points.

### 3.1 Torque estimation

There are several advantages of using a torque model for detecting misfires instead of working directly on the angular velocity signal. To start with, the physical behavior of combustions can be described in a torque model and thus the effects of a misfire can be isolated by theoretical analysis [11]. Another benefit is that the torque has resembling values at similar operating points, which is an advantage in a model-based diagnosis compared to the original angular velocity signal that is more varying, see Figure 2.1.

Various different methods to estimate the engine torque are proposed in the literature, each with their respective advantage. Although a complex model of the crankshaft, such as presented in [17] and [19], would describe the physical behavior more accurately, these methods are not suitable for online misfire detection due to the limited computational power. Instead a simpler model is sufficient to capture the misfire behavior for the purpose of online detection [12]. Using Newton's second law of motion the relation between the torque at crankshaft and the angular velocity can be described as

$$J \frac{d\omega}{dt} = T_{comp} \quad (3.1)$$

where  $J$  is the moment of inertia,  $\omega$  is the angular velocity at the flywheel and  $T_{comp}$  is the composite torque applied on the crankshaft. The inertia depend on  $\theta$  but is here assumed constant.

As the flywheel angular velocity is sampled angular synchronous with a fixed angular interval  $\Delta\theta$  on the flywheel, the left side of (3.1) is modified accordingly

$$J \frac{d\omega}{dt} = J \frac{d\omega}{d\theta} \frac{d\theta}{dt} = J \frac{d\omega}{d\theta} \omega = \frac{J}{2} \frac{d\omega^2}{d\theta}. \quad (3.2)$$

The derivative can then be approximated using Euler forward as

$$\frac{J}{2} \frac{d\omega^2}{d\theta} \approx \frac{J}{2} \left( \frac{\omega_{\theta+\Delta\theta}^2 - \omega_{\theta}^2}{\Delta\theta} \right), \quad (3.3)$$

and thus the composite torque can be obtained by combining (3.1), (3.2) and (3.3) as

$$T_{comp} = \frac{J}{2\Delta\theta} (\omega_{\theta+\Delta\theta}^2 - \omega_{\theta}^2). \quad (3.4)$$

An example of the estimated composite torque for one engine cycle is shown in Figure 3.1.  $J$  is unknown, but as only the fluctuations in the torque signal are of importance for misfire detection, the actual value of the torque is indifferent, and  $\frac{J}{2\Delta\theta}$  can thus be seen as a constant scaling factor. Thus, there is no unit on the y-axis in the figures of the estimated torque, as the torque plots purposes are mainly to show the fluctuating behaviour.

In Figure 3.1, it can be seen that the signal have a periodic appearance where the four highest peaks corresponds to a cylinder combustion. However, the appearance of the six samples corresponding to each cylinder differ between the cylinders which will be further analyzed later.

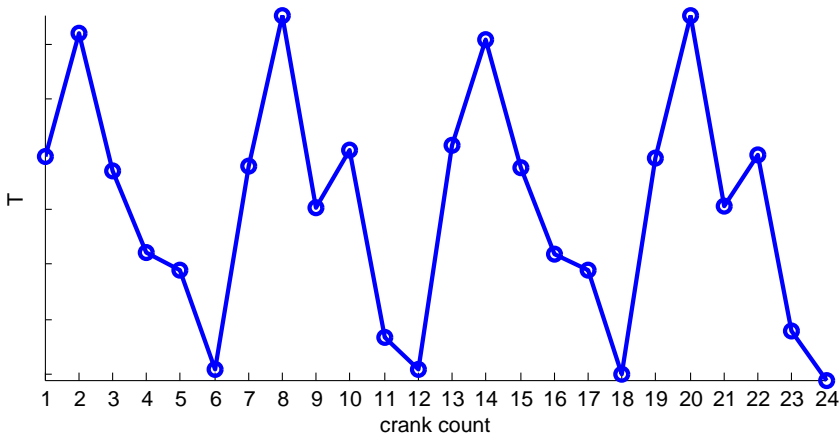


**Figure 3.1:** Estimated torque at 1500rpm and load 0.8g/rev and the corresponding crank counts.

## 3.2 Distinguishing misfire from nominal behavior

The most prominent effect of a misfire is the lack of an in cylinder pressure rise due to the missing combustion. Accordingly, the fluctuations of the corresponding torque produced from the in-cylinder pressure  $T_{pr}$  is the key to detect misfires. An example of how a misfire is visible in the estimated torque signal is shown in Figure 3.2, where the misfire is injected around sample 55.

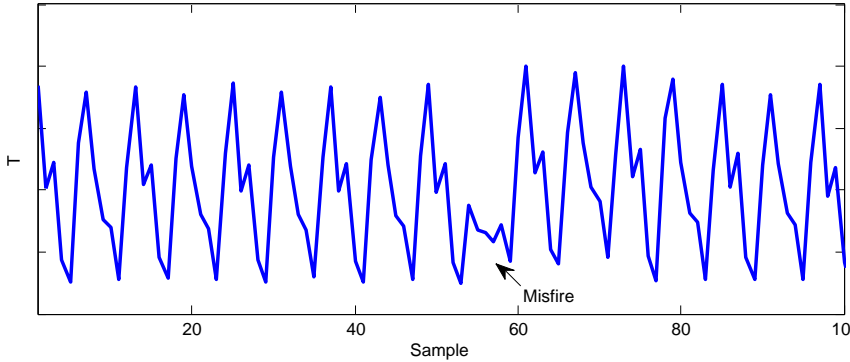


**Figure 3.2:** Estimated torque at 1500rpm and load 0.8g/rev with a visible misfire around sample 55.

However, the torque from the cylinder pressure is only one part of the estimated composite torque  $T_{comp}$  in (3.4) which consist of four main factors

$$T_{comp} = \sum_{i=1}^{n_{cyl}} (T_{pr,i} + T_{mass,i}) - T_{load} - T_{fr} \quad (3.5)$$

where  $T_{pr,i}$  is the torque produced from the in-cylinder pressure in cylinder  $i$ ,  $T_{mass}$  is the inertial torque from the moving piston mass,  $T_{load}$  is the required load from the driveline and  $T_{fr}$  is torque losses due to friction.

If the relatively small dynamic component of the friction is ignored,  $T_{fr}$  may be included in  $T_{load}$  [13]. The composite torque is then reduced to

$$T_{comp} = \sum_{i=1}^{n_{cyl}} (T_{pr,i} + T_{mass,i}) - T_{load}. \quad (3.6)$$

It is known that the fast variations of  $T_{comp}$  are mainly due to  $T_{pr}$  and  $T_{mass}$ , while  $T_{load}$  are less variable within a single stroke [11].

$T_{pr}$  is periodic and largest at the second sample of each combustion i.e. crank count 2, 8, 14 and 20. Thus, in the estimated torque signal, torque peaks related to large  $T_{pr}$  can be observed at these particular crank counts, see Figure 3.1.

$T_{mass}$  changes proportional to  $\omega^2$  and is the dominant factor at higher speed. Ac-

According to [11, 17, 19],  $T_{mass}$  should be periodic just as  $T_{pr}$  and thus similar in each cylinder. However in Figure 3.1,  $T_{mass}$  is proven to have uneven interval in the measurements and is largest at crank count 5, 10, 17, 22. This behaviour probably depend on the engine geometry and is discussed more in the next section.

### 3.2.1 Pre-processing of the estimated torque

Compared to the flywheel velocity signal, the estimated torque has the benefit that at similar speeds and loads it obtain similar magnitudes. This makes it possible to compare different combustions, if they occur at similar speeds and loads. In [12], two steps are presented to pre-process  $T_{comp}$  in order to further distinguish  $T_{pr}$  and to make  $T_{comp}$  independent of load.

**Slow variations** which do not occur during a single stroke is not relevant to detect misfires. Such slow variations include  $T_{load}$  and can be compensated for in the estimated torque,  $T_{comp}$ , by subtracting the mean torque for each engine cycle. This increase the similarity between combustions in each operating point.

**Variation related to load** can be compensated for by normalizing the estimated torque with respect to the air mass introduced per cycle  $m_a$ . This create a quantity that is independent of load but also as demonstrated in [12] the normalization improve performance. Because of the independency of load the considered operating points can be limited to speed and thus significantly reduced.

Remaining characteristics in the estimated torque relies on  $T_{pr}$  and  $T_{mass}$ . In Figures 3.3, 3.4, and 3.5, the normalized estimated torque with subtracted mean are plotted for three different engine speeds, all with a misfire injected in cylinder 1.

The behavior of  $T_{mass}$  prevails at higher speed due to that it changes proportionally to  $\omega^2$  and thereby the torque provided by  $T_{pr}$  is less visually distinguishable. This also means that misfires is less distinct than at lower speed when  $T_{pr}$  is dominant. In Figure 3.4 at 2500rpm,  $T_{pr}$  and  $T_{mass}$  have the same magnitude and two clear peaks are visible for each combustion.

In Figure 3.5, the uneven spacing between the peaks related to  $T_{mass}$  are especially clear. However, as the torque at similar speed has a resembling shape for each cylinder individually, this can be handled by considering each cylinder separately in the algorithm. This also treats the problem with small variations between the different cylinders which might be related to simplifications in the model.

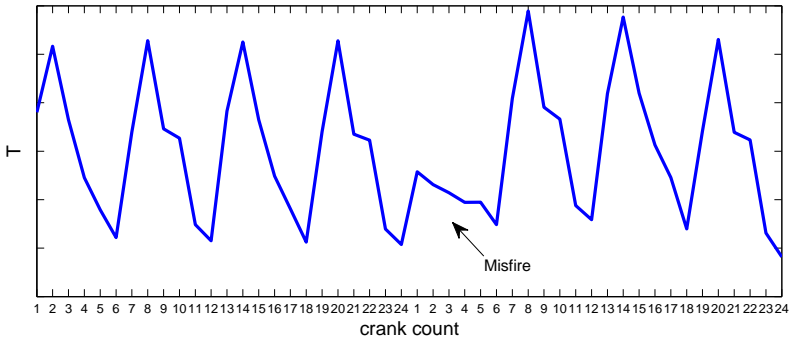


**Figure 3.3:** Estimated torque at 1200rpm with subtracted mean and normalized with respect to  $m_a$ .

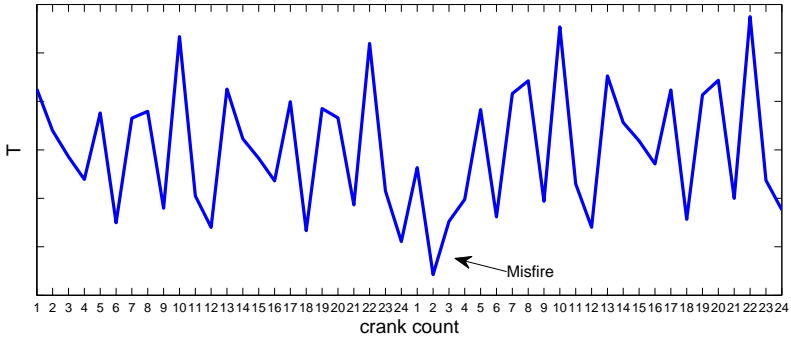


**Figure 3.4:** Estimated torque at 2500rpm with subtracted mean and normalized with respect to  $m_a$ .

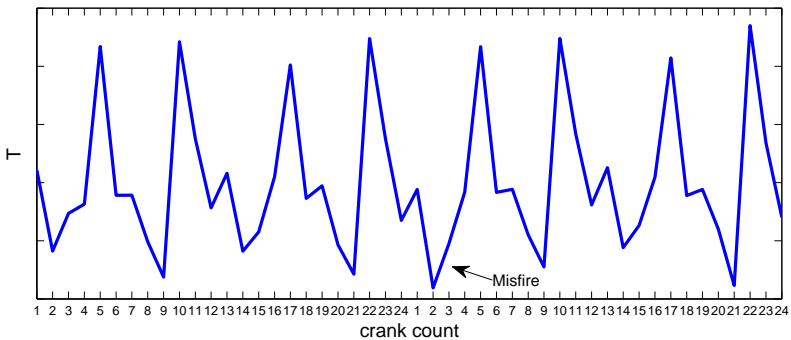


**Figure 3.5:** Estimated torque at 5000rpm with subtracted mean and normalized with respect to  $m_a$ .

### 3.3 Cold starts

The developed engine model is also valid during cold starts and an example of normalized estimated torque with subtracted mean for each cycle during cold start is presented in Figure 3.6. Focus during cold starts is to heat the catalytic converter, the fuel mixture and ignition timing is thereby changed. This causes that  $T_{pr}$  is not as distinct as during normal engine behaviour at the same speed, and the smaller contribution from  $T_{pr}$  makes misfire detection especially difficult during cold starts. As the behaviour during cold starts differ significantly from normal behaviour at the same operating point, cold starts are considered separately when detecting misfires.

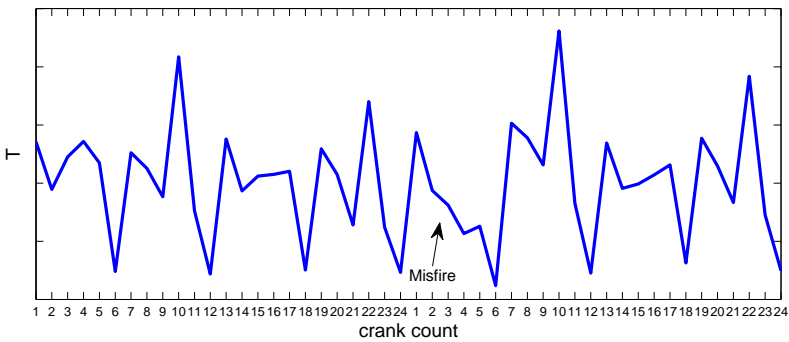


**Figure 3.6:** Estimated torque during cold start at 1200rpm with subtracted mean and normalized with respect to  $m_a$ .

# 4

---

## Misfire detection algorithm

In the design of the misfire detection algorithm, the purpose is to create a test quantity that classify each combustion as either a misfire or a fault-free combustion. The algorithm design used in [12] for six cylinder vehicles is here used with only minor changes as a result of the cylinder reduction. The algorithm design includes the creation of a test quantity which attempt to optimally use all crank counts assigned to each cylinder in order to determine the combustion behavior.

### 4.1 Operating points

The estimated torque has proven to have a varying behaviour and as previously suggested, data need to be categorized depending on the actual engine operating conditions. As the normalization with respect to air mass flow per cycle, introduced in Section 3.2.1, remove dependency on load, only varying speed is considered. Nine operating points based on speed are used in this work, starting at 1000rpm with 500rpm intervals up to 5000rpm, where each combustion is associated to the best matching. For example, this means that idling, which occur around 850rpm, is categorized to the lowest operating speed.

To handle the deviations between the cylinders, the estimated torque is further categorized depending on the firing cylinder resulting in: cylinders \* speed operating points = 36 engine modes. Finally also cold start need to be considered separated in the algorithm to ensure better performance. As cold starts are limited to lower engine speeds only the lowest three speed operating points are considered. In total, this result in 48 operating points for four cylinder vehicles where each operating point needs an optimized test quantity to classify data. A similar conducted categorization for a six cylinder engine results in 72 operating points.

## 4.2 Hypothesis test

The behavior of each combustion  $k$  is described by a vector of six samples of the estimated torque,  $t_k = (T_1, T_2, T_3, T_4, T_5, T_6)^T$  corresponding to the firing cylinder. Where  $t_k$  either belong to the behavioral mode of misfire,  $F_{mf}$ , or no fault,  $NF$ .

The behavior of the estimated torque is highly variable. Even though different operating points are used, certain variations within each operating point need to be managed. Since a consistent difference is observed when a misfire occur compared to fault-free behaviour, these smaller variations within each operating point can be handled by considering probability density functions (pdf). For each operating point a hypothesis test can thus be formed where the behavioral modes are described by pdfs.  $p_{nf}$  is the fault-free distribution connected to the null hypothesis and  $p_{mf}$  is the misfire distribution connected to the alternative hypothesis,

$$\delta(t_k) = \begin{cases} H^0 & \text{if } t_k \in p_{nf}(t_k|\omega) \\ H^1 & \text{if } t_k \in p_{mf}(t_k|\omega) \end{cases}$$

where both distributions are dependent of speed. To visualize how  $p_{nf}$  and  $p_{mf}$  may appear, histograms of sample 1 and 4 in cylinder 1 around 1500rpm are shown in Figure 4.1 and Figure 4.2.

## 4.3 Design of test quantity

The detectability performance of a misfire vary between the different samples associated to a combustion, which is clear when comparing the separation of misfires and fault-free combustions in Figure 4.1 and Figure 4.2. However, in the creation of the test quantity as much information about each combustion as possible is wanted. Thus all six samples are used while emphasis is placed on the samples with greater separation.

A straight forward way of doing so is to assign weights to the samples based on how much information they include, and thereby take all samples into consideration [12]. The aim is to choose weights such that the resulting one-dimensional test quantity has as large separation between the distributions of misfire and fault-free combustions as possible. Further, this method is suitable for online diagnosis as it is not computationally complex.

If  $w_k = (w_1, w_2, w_3, w_4, w_5, w_6)^T$  is the weights for a certain operating point  $k$ , the test quantity  $r$  is given by

$$r = w_k^T t_k + \beta_k \quad (4.1)$$

where  $t_k = (T_1, T_2, T_3, T_4, T_5, T_6)$  is the normalized estimated torque with removed mean for one combustion categorized to operating point  $k$ .  $\beta_k$  is chosen in each operating point such that  $r \geq 0$  in the fault-free case and  $r < 0$  for misfires. This

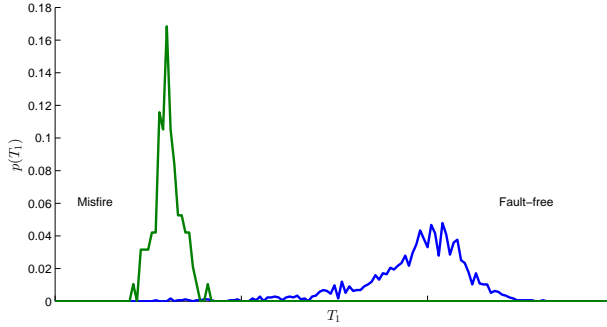


**Figure 4.1:** Histogram of estimated torque from sample 1 in cylinder 1 around 1500rpm

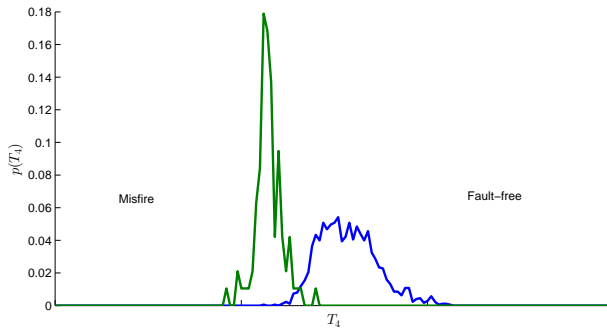


**Figure 4.2:** Histogram of estimated torque from sample 4 in cylinder 1 around 1500rpm

means that  $\beta_k$  works as a threshold and a higher value increase the risk of false alarms while the risk of missed detection is decreased and the other way around when  $\beta_k$  is lowered.

## 4.4 Parameterization

The weights  $w_k$  and the threshold parameter  $\beta_k$  are found and stored in the algorithm using training data. This means in each operating point, 7 parameters needs to be stored in four cylinder vehicles, respectively, 5 parameters in the six cylinder vehicles. In total, for all operating points, this results in that 336 parameters needs to be stored in a four cylinder vehicle and 360 parameters in a six cylinder vehicle.

To find the parameters that maximize the separation between the fault-free pdf and the pdf of misfire in each operating point, the machine learning approach Support Vector Machines (SVM) is utilized. SVM is a technique developed for

binary classification and can be applied to parameterize models such as the one described by (4.1), see [2].

SVM used training data and the approach may roughly be interpreted as maximizing the margin between the two classes' closest data points, denoted as the support vectors. The support vectors contain all relevant information about the classification and thereby only the closest data points are relevant. The middle of the margin is by SVM considered the optimal decision boundary that separates the two classes. If the distributions of the two classes overlap, data points on the "wrong side" of the boundary are penalized to reduce their influence in the optimization. For further information about SVM see [2] and [9].

The requirements in Volvo KPI places emphasis on avoiding false alarms rather than avoiding missed detections, which will be further declared in Section 5.2. Thus, the middle of the margin is not the optimal decision boundary in this application. However, to avoid manual calibration of the threshold in each operating point, the thresholds selected by SVM are used in this work.

## 4.5 Summary

All the necessary tools to set up the misfire detection algorithm are now presented and as a summary, the steps to train the algorithm are described below. All parameters are automatically tuned with no need for manual calibration.

1. Use training data that cover all considered engine operating points where both fault-free data and misfire data have to be included. Estimate the torque and compensate for unwanted variations by removing the mean torque for each engine cycle and normalize the estimated torque with respect to air mass introduced per cycle  $m_a$ .
2. Categorize each combustion in operating points based on speed, firing cylinder, if cold start occurs or not and if the combustion belongs to the fault-free case or misfire. Crank counts in Table 2.3 are used to associate the correct samples to each cylinder.
3. Parameterize the weights and thresholds in the test quantity for each operating point with the use of SVM.

# 5

---

## Kullback-Leibler divergence correlated to Volvo KPI

A method to quantify the separation between the pdf of misfire and the pdf of fault-free combustion is interesting for analysing the diagnosis performance. For this purpose the Kullback-Leibler divergence is introduced in this chapter. The Kullback-Leibler divergence give a good basis for evaluation and comparison. However, without any connection to the actual requirements on the detection algorithm specified in Volvo KPI, the Kullback-Leibler divergence does not provide any explicit information about the algorithm performance. By establishing a correlation between the Kullback-Leibler divergence and the requirements, the application of the Kullback-Leibler divergence is increased to also include evaluating if requirements can be met.

### 5.1 Kullback-Leibler divergence

The Kullback-Leibler divergence is a tool used in probability theory, information theory and statistics to measure the similarity between two density functions [10]. The Kullback-Leibler divergence from misfire data  $p_{mf}$  to fault-free data  $p_{nf}$  is expressed  $K(p_{mf} \parallel p_{nf})$  and defined as

$$K(p_{mf} \parallel p_{nf}) = \int_{-\infty}^{\infty} p_{mf}(x) \log \frac{p_{mf}(x)}{p_{nf}(x)} dx \quad (5.1)$$

where

$$K(p_{mf} \parallel p_{nf}) \geq 0 \text{ and}$$

$K(p_{mf} \parallel p_{nf}) = 0$  only if  $p_{mf} = p_{nf}$ ,

which can be interpreted as the expected log-likelihood ratio when  $p_{mf}$  is the true distribution [12].

In [12] it is suggested to use the Kullback-Leibler divergence to quantify the separation of two pdfs to evaluate the detection performance in fault diagnosis. It may then instead be interpreted as the "distance" between faulty data and fault-free data, where a higher value means larger separation between faulty data and fault-free data i.e., it is easier to distinguish  $p_{mf}$  from  $p_{nf}$ .

For an accurate calculation of the KL divergence the estimation of the pdfs is important. Especially the estimation of the tail of  $p_{nf}$  is crucial since if the pdfs are well separated, the computation of (5.1) mainly depends on the tail of  $p_{nf}$  since  $p_{mf}$  is close to zero for fault-free data. There are various ways the pdf could be approximated. Either a non-parametric method e.g. a kernel density estimator can be used, which center a kernel function at each data point and then approximate the pdf by summing up all the kernel functions [2], or a parametric method, which fits a known distribution to data by estimating its parameters [3].

A non-parametric method requires lots of data to make a good approximation of the tails and is in the computation of the Kullback-Leibler divergence very sensitive to outliers. As the distribution of fault-free and misfire data has an appearance similar to the normal distribution, see Figure 4.1 and Figure 4.2, a parametric Gaussian distribution is used as an approximation in this work. In addition, the requirements on the diagnosis algorithm are partially expressed in standard deviations based on Gaussian distributed data.

If  $p_{nf}$  and  $p_{mf}$  are  $k$ -dimensional multivariate Gaussian distributions, respectively, with mean  $\mu_{p_{nf}}$  and  $\mu_{p_{mf}}$ , and covariance matrix  $\Sigma_{p_{nf}}$  and  $\Sigma_{p_{mf}}$ . The Kullback-Leibler divergence can be computed analytically as

$$K(p_{mf} \parallel p_{nf}) = \frac{1}{2} \left( \text{tr}(\Sigma_{p_{nf}}^{-1} \Sigma_{p_{mf}}) + (\mu_{p_{nf}} - \mu_{p_{mf}})^T \Sigma_{p_{nf}}^{-1} (\mu_{p_{nf}} - \mu_{p_{mf}}) - \log \left( \frac{\det \Sigma_{p_{mf}}}{\det \Sigma_{p_{nf}}} \right) - k \right) \quad (5.2)$$

## 5.2 Volvo KPI

Volvo KPI include requirements on probability of false alarm and probability of missed detection which both depend on the threshold placement. First priority for a manufacturer when thresholding misfire detection algorithms, is to meet the requirements in the OBDII legislation regarding detecting misfires, in order to get legal permission to sell the vehicle. The requirement on highest probability of missed detection related to the OBDII legislation depend on several factors [1]. Here an approximation is used, for a simpler interpretation, and the demand is

	Min.dist. to J	Max.misclass. [%]
False alarm	$4.2\sigma_{nf}$	0.0058
Missed detection	$2.7\sigma_{mf}$	1

**Table 5.1:** Requirements on the detection algorithm in terms of false alarm and missed detection, expressed both as the minimum allowed distance in standard deviations from the mean to the threshold  $J$ , and maximum allowed percentage of misclassification.

set such that at least 99% of occurred misfire must be detected. From the manufacturer's point of view, this requirement is adequate to avoid vehicle damage due to not detected misfires and therefore the main focus is instead on avoiding false alarms.

False alarms increase the risk for unnecessary warranty issues that could lead to high costs for a manufacturer. Thus the requirement on the probability of false alarm, which is set by the manufacturer, is more stringent than the requirement on probability of missed detection.

The requirement in Volvo KPI is set with the premise that the threshold used for classification  $J$  is selected such that the legal requirement on probability of missed detection is met. Based on this threshold placement, the requirement on probability of false alarms are expressed as the distance between the mean of the fault-free data  $\mu_{nf}$  and  $J$ , measured in standard deviations of the fault-free data  $\sigma_{nf}$ . The requirement is set to a minimum distance of  $4.2\sigma_{nf}$  between  $\mu_{nf}$  and  $J$ . In the requirement both the distribution of fault-free data  $p_{nf}$  and misfire data  $p_{mf}$  are assumed to be Gaussian with means  $\mu_{nf}$  and  $\mu_{mf}$ , and variance  $\sigma_{nf}^2$  and  $\sigma_{mf}^2$ .

In Table 5.1 the requirements are presented, both expressed in the maximum allowed percentage of misclassification and the minimum allowed distance in standard deviations. The distance between  $p_{mf}$  and the  $J$ , is measured in standard deviations of the misfire data  $\sigma_{mf}$ .

The minimal distance between the mean of  $p_{nf}$  and the mean of  $p_{mf}$  that meet the requirements, can therefore be expressed  $(4.2\sigma_{nf} + 2.7\sigma_{mf})$ . This distance is visualized in Figure 5.1, where also the threshold is selected such that both the requirement on probability of false alarms and the requirement on probability of missed detection are meet.

### 5.3 Correlation

The Kullback-Leibler divergence use no information about the threshold in its equation (5.2), while both the requirement on the probability of missed detection and the probability of false alarm are dependent on the threshold position. However, if both requirements is considered together, the position of the thresh-

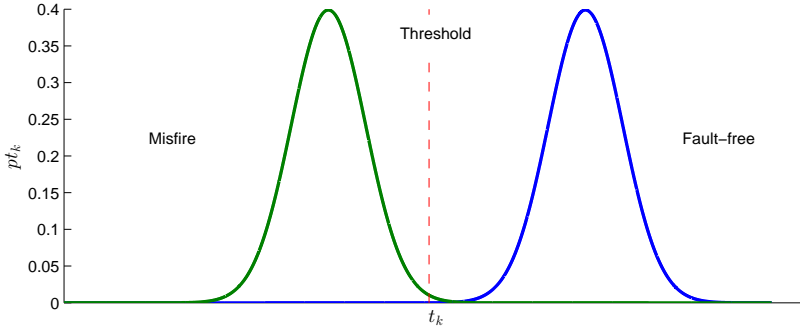


**Figure 5.1:** Gaussian pdfs with minimal separation that meet the requirements and the threshold inserted  $4.2\sigma_{nf}$  from  $\mu_{nf}$  and  $2.7\sigma_{mf}$  from  $\mu_{mf}$

old can be ignored and a correlation between the Kullback-Leibler divergence and the requirements in Volvo KPI can be established.

By replacing the distance between the distribution means ( $\mu_{p_{nf}} - \mu_{p_{mf}}$ ) in equation (5.2) in the one-dimensional case, with the corresponding minimum distance in the requirement ( $4.2\sigma_{nf} + 2.7\sigma_{mf}$ ). A lower limit of the Kullback-Leibler divergence that meet the requirements can be obtained.

$$K(p_{mf} \parallel p_{nf}) = \frac{1}{2} \left( \frac{\sigma_{mf}^2}{\sigma_{nf}^2} + \frac{(4.2\sigma_{nf} + 2.7\sigma_{mf})^2}{\sigma_{nf}^2} - \log \frac{\sigma_{mf}^2}{\sigma_{nf}^2} - 1 \right) \quad (5.3)$$

which can be written as

$$K(p_{mf} \parallel p_{nf}) = 4.15\sigma_R^2 + 11.35\sigma_R - \log \sigma_R + 8.32 \quad (5.4)$$

where  $\sigma_R = \frac{\sigma_{mf}}{\sigma_{nf}}$ .

Thus, the lowest value of the Kullback-Leibler divergence that fulfill the requirements in Volvo KPI depends on the ratio between the standard deviations of the two distributions. In Figure 5.2, it is shown how the limit change depending on the ratio where the calculated Kullback-Leibler divergence between fault-free and misfire data should be equal or larger than the values given by the curve to meet the requirements. The curve starts at Kullback-Leibler divergence 11.8 and a standard deviation ratio of 0.1.

Data used in this work normally have a ratio that vary between 0.1 and 1 at speeds below 2500rpm and a slightly higher ratio up to 2 at higher speeds. This could depend on that less data are available at higher speed, especially during misfire which lead to a higher standard deviation and thus the ratio is larger. In Chapter 7 the computed ratios and Kullback-Leibler divergence from the test quantities in the algorithm are presented and the evaluation with this method is further discussed.

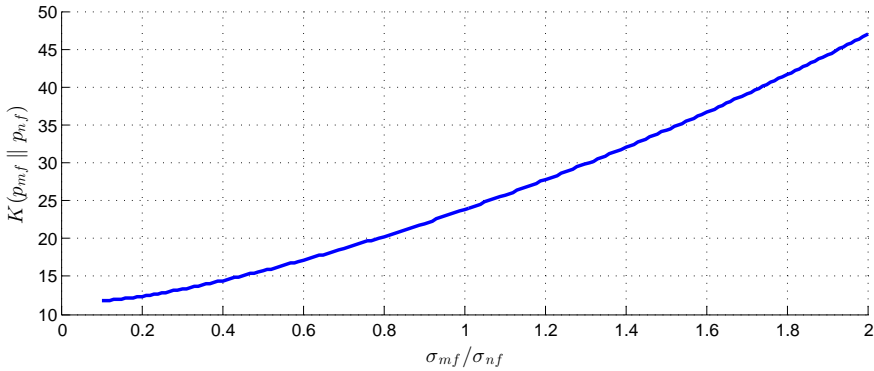


**Figure 5.2:** The lowest allowed Kullback-Leibler divergence between the distribution of fault-free and misfire data, that is able to fulfill the requirements, as a function of the ratio of standard deviations between misfire data and fault-free data.

This correlation between the Kullback-Leibler divergence and the requirements in Volvo KPI assumes that the threshold will be set in the optimal location in relation to the set demands and that the approximation of the Gaussian distributions are valid. In the data sets 1-3 which are following the FTP75 city driving cycle and in data set 4 measured on the road, few data points for misfire are available at higher engine speeds due to limited driving in these conditions. Thereby the Gaussian approximation of the misfire distribution might not be valid, and the evaluation with the Kullback-Leibler divergence at higher engine speed is considered uncertain.

## 5.4 Conclusion

The Kullback-Leibler divergence as an evaluation tool has several advantages that have been presented in this chapter. Compared to evaluation using only the requirements, the Kullback-Leibler divergence is not limited to use with Gaussian distributions. However, to relate Kullback-Leibler divergence to the requirements in Volvo KPI, approximated Gaussian distributions is here used. In the computation of the Kullback-Leibler divergence, the approximation of the distributions tails is central, since a rapid decaying tail result in values that quickly tends infinity. Although the cases that result in infinity can be interpreted as good enough, but then there is no basis for comparison and analysis which is the whole idea behind the use of the Kullback-Leibler divergence in this application. Another advantage of using the Kullback-Leibler divergence is that no knowledge about the threshold is needed, only the separation between the two pdfs is considered. Since information from both pdfs are used, correlation to both the demand on detected misfires and the allowed number of false alarms can be drawn. This enables that the same tool can be used both during development and as a evalu-

ation of the algorithm. The correlation also enables evaluation, connected to the requirements, earlier during the development process.

Further the Kullback-Leibler divergence allows computation in higher dimensions but the correlation to the requirements is only established in one dimension. Therefore when multiple dimensions are considered in this work, the computed Kullback-Leibler divergence is used for comparison only and not to investigate if the requirements in Volvo KPI are met.

# 6

---

## Robustness analysis of misfire detection algorithm

To investigate how the misfire detection algorithm handles variations and to better understand how the estimated torque varies due to varying measurement conditions, a robustness analysis of data from several vehicles is conducted in this chapter. The analysis covers how the estimated torque and misfire detectability varies between vehicles with different engine configurations and how different vehicles with same engine configuration vary among themselves. A solution is proposed on how to compensate for vehicle to vehicle variations such as manufacturing errors. In addition, the problem with torsional vibrations in the crankshaft after a misfire is addressed and a model-based solution is proposed.

### 6.1 Varying number of cylinders

Recently at Volvo, a new generation of engines with four cylinders was introduced instead of the previous generations with five or six cylinders. This of course affects the vehicle in various ways and the subsequent changes crucial for misfire detection is examined in this section. The detection algorithm in [12], which this work is based upon, was developed using data from a six cylinder engine and thus it is important to understand how the detectability performance is affected when the number of cylinders are reduced.

A valid comparison is difficult to perform since data collected in real driving scenarios are affected by varying environmental influences and driver operation. Therefore, all data used in this comparison is collected in a chassis dynamometer under controlled conditions. An example of the estimated torque from a six cylinder vehicle is shown in Figure 6.1 which can be compared with the four cylinder measurements in Figure 3.1 collected at the same speed and load.

During one engine cycle, two additional cylinder combustion occurs which gives

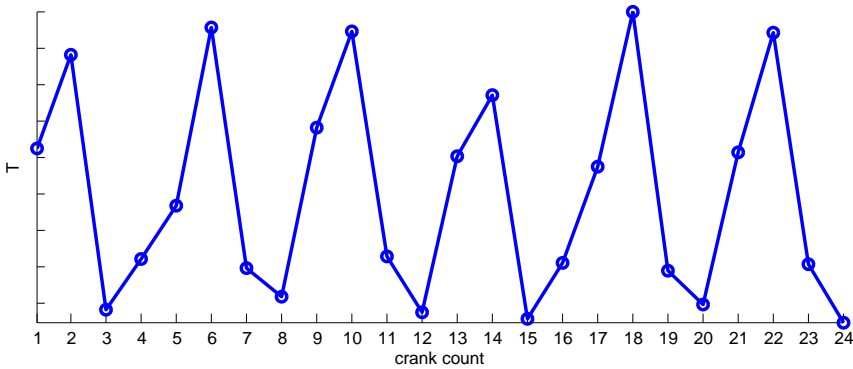


**Figure 6.1:** Estimated torque at 1500rpm and load 0.8g/rev and the corresponding crank counts in a six cylinder engine.

two additional torque peaks. Compared to the four cylinder engine no uneven spacing between the peaks from the reciprocating torque is observed.

### 6.1.1 Misfire Visibility

To analyze the misfire visibility in a four cylinder engine compared to in a six cylinder engine, data collected at one fixed speed and load is used. Figure 6.2 and Figure 6.3 display several fault-free combustions and misfires plotted in the same figure, from two such stationary operating points for both engine types. Each figure contains data from one cylinder. The plots to the left show estimated torque from the four cylinder engine and the plots to the right show estimated torque from the six cylinder engine.

Furthermore the Kullback-Leibler divergence is computed for each crank count in the figures individually, to quantify the separation and the results are presented in Table 6.1 and 6.2.

In all figures, misfires are well separated from fault-free data. The separation is greatest at the crank counts where the combustion provide most torque and less distinct when the slower changing torque from the inertia is big. In the four cylinder engine, the peaks from the inertial torque comes with uneven intervals which was observed in Section 3.3. Therefore two different appearance are observed in cylinder 1 and 2. For the same reason, the behaviour of cylinder 4 is similar to cylinder 1 and cylinder 3 have a similar behaviour to cylinder 2, see Figures 3.3, 3.4, and 3.5.

At lower speeds, the torque contribution from the inertia is smaller and the effects from a combustion is visual longer i.e. misfires are separated from fault-free data during more samples. Comparing the plots from the two engine configurations at low speed, a similar behaviour is displayed in both cases. However, in the four cylinder engine where there are longer time between the combustions more samples are clearly separated. Interesting to observe is sample 6 in the four

		Cylinder 1					
Engine model	Sample						
1500rpm	1	2	3	4	5	6	
4 cyl	16.69	379.25	100.64	31.15	1.10	11.88	
6 cyl	57.41	178.54	60.07	10.65			
4000rpm							
4 cyl	17.02	163.34	27.23	0.01	2.55	8.21	
6 cyl	0.73	30.24	13.61	0.12			

**Table 6.1:** Kullback-Leibler divergence for each crank count in Figure 6.2.

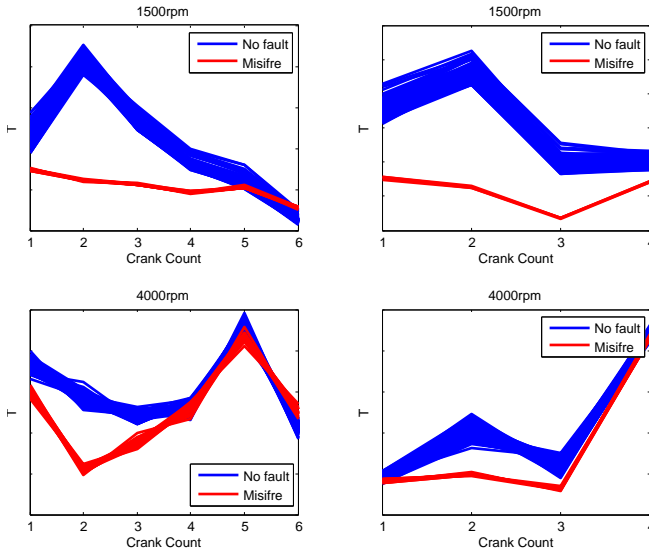


**Figure 6.2:** Estimated torque from cylinder 1 at 1500rpm and 4000rpm. The two plots to the left are from a four cylinder engine and the two to the right are from a six cylinder engine.

cylinder engine where the estimated torque of misfire are slightly higher than the fault-free values.

Considering the computed Kullback-Leibler divergence in Tables 6.1 and 6.2, at least one of the samples in each configuration and cylinder is well above the requirements stated in Section 5.2 as  $\sigma_{mf}/\sigma_{nf}$  is below 1 in all cases. This means that if the detection algorithm is designed in an efficient way the requirements should be met. However, note that this is steady state data in which it is considerably easier to separate the distributions compared to more varying conditions. Comparing the six and four cylinder engine, the values indicates that misfires are more separated from fault-free data in the four cylinder engine, and at least the last of the two additional samples should improve the detectability of misfires.

Cylinder 2						
Engine model	Sample					
1500rpm	1	2	3	4	5	6
4 cyl	6.37	174.09	34.08	10.12	3.06	12.94
6 cyl	40.10	201.57	38.42	3.18		
4000rpm						
4 cyl	14.34	117.37	15.37	0.72	0.28	7.58
6 cyl	1.20	39.05	12.60	0.65		

**Table 6.2:** Kullback-Leibler divergence for each crank count in Figure 6.3.

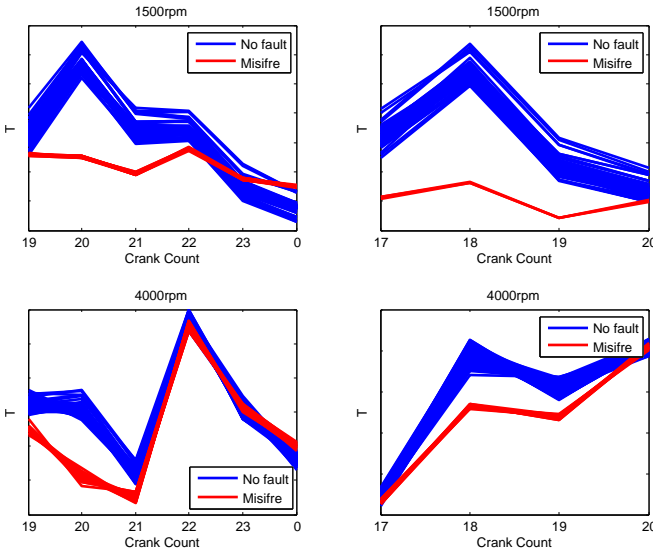


**Figure 6.3:** Estimated torque at cylinder 2 at 1500rpm and 4000rpm. The two plots to the left are from a four cylinder engine and the two to the right are from a six cylinder engine.

The different behavior of cylinder 1 and 2 in the four cylinder engine are proven to give different performances as cylinder 2 obtain significantly lower values.

At higher speeds the inertial torque prevail and thereby the distinguishability of a misfire is reduced in the plots. In both engine configurations, the clearest reduction in estimated torque following a misfire passes before the next combustion occur, and the estimated torque obtain the same magnitude as in the fault-free case. However, misfires are still separated in the sixth sample in the four cylinder engine as the estimated torque of misfire become larger than in the fault-free case. The computed Kullback-Leibler divergence still indicates that the requirements should be met and that in the four cylinder engine misfires are still more detectable in cylinder 1 than cylinder 2.

It is important to consider the varying detectability between the samples during a combustion when the detection algorithm is designed. For a better comparison of the overall performance, all samples assigned to a cylinder need to be considered together.

### 6.1.2 Misfire detectability performance

To get an overview of the misfire detectability for the different cylinders and engine configurations, the Kullback-Leibler divergence can be computed for all samples assigned to one cylinder. Data from varying speeds and loads are used and divided into operating points depending on speed and cylinder, see Table 6.3 for the six cylinder engine and Table 6.4 for the four cylinder engine. However higher dimensions are used for the computation of the Kullback-Leibler divergence and thus the relation to the requirements established in Section 5.2 can not be applied. The load are varied over an equidistant range at each speed except 1000rpm in the six cylinder engine where less data was available.

The result indicates that in the six cylinder engine it should be most difficult to detect a misfire around 1500rpm and with increased difficulty for cylinders further away from cylinder 1. Important to note is that the data used in the computation had less varying load at 1000rpm which probably is the reason to the high values, which coincides with the results in [5]. When the speed increases the separation also increases. This partly contradicts the results in previous section when each sample was considered. The explanation is that at higher speeds, the distance between the mean of the estimated torque of misfires and fault-free data, at the most separated samples, are larger than at lower speeds. However when consid-

Cylinder	Speed [rpm]							
	1000	1500	2000	2500	3000	3500	4000	4500
1	249.15	51.51	86.11	66.73	122.31	172.29	167.86	144.34
2	248.67	51.08	88.38	63.51	122.00	169.43	162.73	135.05
3	224.18	50.76	81.83	64.35	116.86	166.62	151.41	121.35
4	241.65	50.85	82.63	62.36	120.94	181.39	159.32	111.77
5	183.03	52.04	79.54	57.66	121.03	168.69	147.85	135.62
6	273.13	48.32	77.41	57.24	109.46	137.10	138.52	133.02

**Table 6.3:** Kullback-Leibler divergence for all cylinders at various speed and load in a six cylinder engine.

Cylinder	Speed [rpm]							
	1000	1500	2000	2500	3000	3500	4000	4500
1	92.36	134.33	115.59	152.63	145.47	136.93	151.84	183.42
2	52.36	71.41	43.71	75.46	95.38	75.25	97.01	115.58
3	70.57	118.22	100.86	117.42	113.85	94.45	119.87	148.04
4	85.26	117.64	56.25	76.75	76.20	73.31	89.17	90.24

**Table 6.4:** Kullback-Leibler divergence for all cylinders at various speed and load in a four cylinder engine.

ering steady state data, at one crank count with constant speed and load, the variances are very small especially at lower speeds and thus the Kullback-Leibler divergence become higher. When more varying data are used, the distance between the distribution means are still similar but the variances have increased, which give a larger impact in the Kullback-Leibler divergence at lower speed.

The result from the four cylinder engine is more difficult to interpret. Certain trend with decreasing detectability following the firing order can be observed as cylinder 1 and 3 have the highest Kullback-Leibler divergence and cylinder 4 and 2 have the lowest values.

Comparing the different speed operating points there are no clear trend but the results suggest that both 1000rpm and 2000rpm are especially problematic.

Based on these results, there are no clear benefits of the reduced number of cylinders. Although the additional two samples associated with each cylinder shows further information about the misfire. The four cylinder vehicle has a considerable variation between the cylinders as it both contains the cylinder with largest and smallest separation between fault-free data and misfire data.

The only significant observed difference between the cylinders that which could explain this is the behaviour of the inertia torque. To obtain similar values in each cylinder a more complex model that describe the inertia torque and other torsional effects are required but at a higher computational cost.

Since each cylinder is considered separately, the model is still useful and the use of the misfire detection algorithm developed in [12] is valid.

## 6.2 Vehicle to vehicle variations

The measurement of the angular velocity at the flywheel is central in the detection of misfires. In the previous equations in Section 2.2.1, the production of the flywheels is assumed to be perfect with no manufacturing errors at all. Even if the margin of error in the production is small, it is suggested in [19] that manufacturing errors such as tooth errors on the flywheel exist and affect the measurements. Similar issues may also emerge with wear out of the teeth on the flywheel [15].

In a model-based approach where training data is used, periodic errors in the signal due to the manufacturing may not be a problem if the algorithm is only trained and used on one specific vehicle. However to accurately use the algorithm on several objects, manufacturing errors must be considered.

### 6.2.1 Pitch error modeling

In [19], manufacturing errors are modeled by adding a teeth pitch error  $b_\theta$  to the angular velocity  $\omega$  equation (3.2) as

$$\omega_i = \frac{\Delta\theta + b_\theta}{\Delta t_i} \quad (6.1)$$

where  $\Delta\theta$  is the fixed interval between two teeth and  $\Delta t_i$  is the measured time between two samples. When  $30^\circ$  measurement resolution is used,  $b_\theta$  is a vector with values for 12 angular intervals and thus cover a full revolution. Each parameter in the vector  $b_\theta$  is used twice during every engine cycle as the flywheel rotates two revolutions. Since all measurements to estimate the torque are taken from this signal, the teeth pitch error implicit comprise all systematic distortions.

To visualize how the estimated torque may vary when the described errors exist, an error ( $b_\theta = -0.05^\circ$ ) is introduced in the data according to (6.1) at crank count 21, and plotted together with the original data in three dimensions, see Figure 6.4. Values belonging to misfires are marked as "+". The three dimensions belong to the crank counts with most separation between fault-free and misfire data of cylinder 2 i.e. crank counts 19, 20 and 21.

To visualize the approximated Gaussian distributions of data and also show the requirements, ellipses representing 4.2 standard deviations for the fault-free data and 2.7 standard deviations for misfires are plotted for each 2D projection of the data. Again, the used data is collected in a chassis dynamometer and the different groups in the plot comes from the varied load.

The introduced error produce a distinct displacement that decreases when the load increase and is especially clear at the projection at the  $T_2 - T_3$  plane. A similar behavior is observed at both operating speeds since the error changes proportional to engine speed. Due to the displacement the fault-free distribution of vehicle 1 and the misfire distribution of the vehicle with introduced pitch error partially coincide. This means that if a misfire detection algorithm trained with data from vehicle 1 was used on the vehicle with introduced pitch error, there

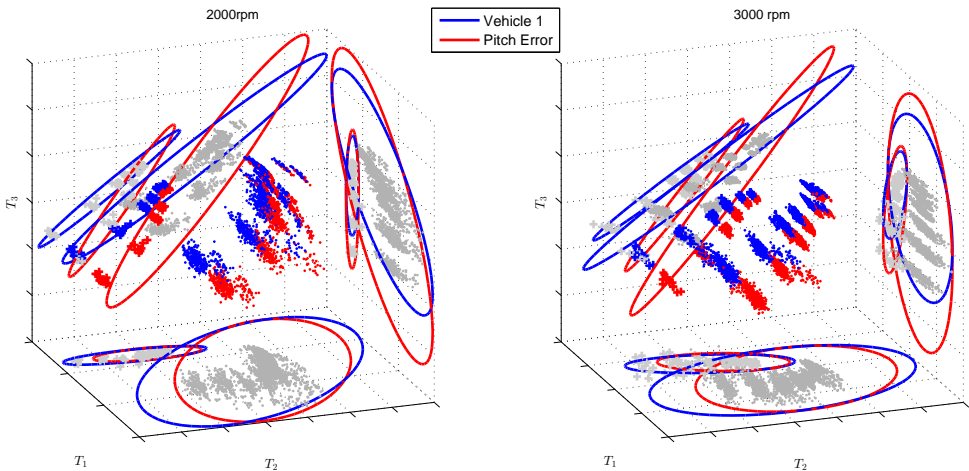


**Figure 6.4:** Estimated torque at crank count 19 ( $T_1$ ), 20 ( $T_2$ ) and 21 ( $T_3$ ). Values which belongs to misfires are marked as "+". The ellipses around the projections on the different axes represent the requirements.

would be a raised risk for missed detections.

To investigate if these kind of variations are present between real vehicles, data from vehicle 2 and vehicle 3 in Table 2.1 is compared in Figure 6.5.

A constant offset can be observed in between the vehicles both plots, even if not as clear as in Figure 6.4 with an introduced error. The displacement is especially visible in the 2D projection at the  $T_2 - T_3$  plane with a rotation between the distributions at both engine speeds, marked in the plots with a dashed circle. Such recurrent offset between vehicles can be explained by teeth pitch errors or other factors that are included in (3.2).

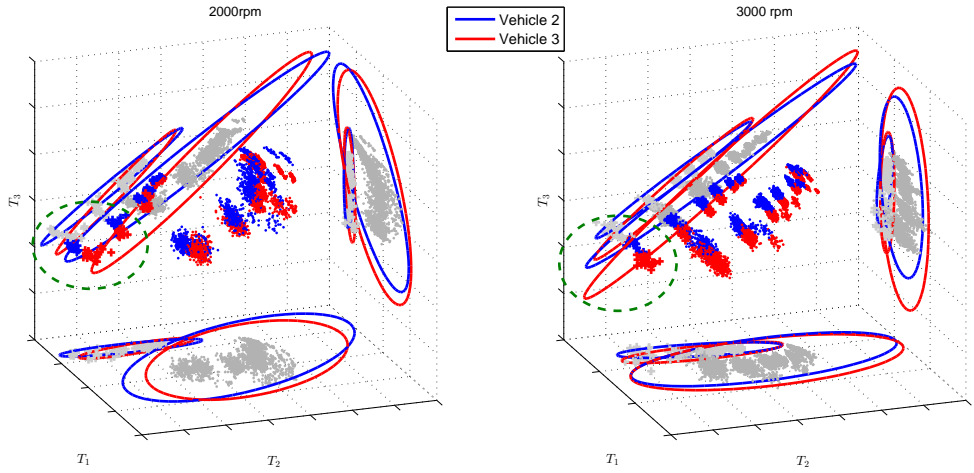


**Figure 6.5:** Estimated torque at crank count 19 ( $T_1$ ), 20 ( $T_2$ ) and 21 ( $T_3$ ). Values which belongs to misfires are marked as +. The ellipses around the projections on the different axes represent the requirements.

## 6.2.2 Compensation

To be able to compensate for constant variations between vehicles as the one described above, it is sufficient to find  $b_\theta$  in equation (3.2). The correction factor  $b_\theta$  between vehicle 2, here considered as the true vehicle, and vehicle 3 is estimated by using equations (6.1) and (2.1)

$$\frac{\Delta\theta}{\Delta t_{i,2}} = \frac{\Delta\theta + b_\theta}{\Delta t_{i,3}} \quad (6.2)$$

which can be rewritten as

$$b_\theta = \Delta\theta \left( \frac{\Delta t_{i,3}}{\Delta t_{i,2}} - 1 \right) \quad (6.3)$$

where  $\Delta t_{i,2}$  and  $\Delta t_{i,3}$  are the segment times at interval  $i$  for vehicle 2 and 3.

The difficulty in estimating  $b_\theta$  is to avoid that temporary variations are included

in the estimation. The segment time measurements used in (6.3) are in the same way as the angular velocity measurements highly varied which creates difficulties when two measurements are compared. To conduct the comparison between similar data and avoid variations due to change in speed and load as well as environmental conditions, steady state measurements at constant speed and load are used from both vehicles in the computation. The parameter  $b_\theta$  is then estimated by using the mean value at each crank count for several measured engine cycles with removed trends. Since each segment on the flywheel is measured twice, the mean segment time ratios from the two revolutions are used. Furthermore measurements at higher speeds are preferred in the estimation as the variations due to engine geometry are clearer in measurement. Since  $b_\theta$  is a constant, values obtained at one operating point can then be used at all operating points.

The obtained values of  $b_\theta$  when the vehicles in Figure 6.5 are considered, lies between  $-0.0375^\circ$  and  $+0.024^\circ$ . This magnitude of the errors is consistent with results presented in [19]. For further validation,  $b_\theta$  computed with (6.3) is used to calibrate data from vehicle 3 against vehicle 2. The result is presented in Figure 6.6. At both speeds, the calibration increases the similarity between the vehicles which should improve the diagnosis performance.

The compensation is further evaluated with the Kullback-Leibler divergence in Section 7.3, where the compensation is implemented in the detection algorithm. The implementation in the misfire detection algorithm is done by storing the mean estimated torque for each crank count from a steady state measurement at one operating point, thereby totally 24 extra parameters needs to be stored. Before the algorithm is used, this data is utilized to find the compensation vector  $b_\theta$  that then is used in the angular velocity measurements (6.1).

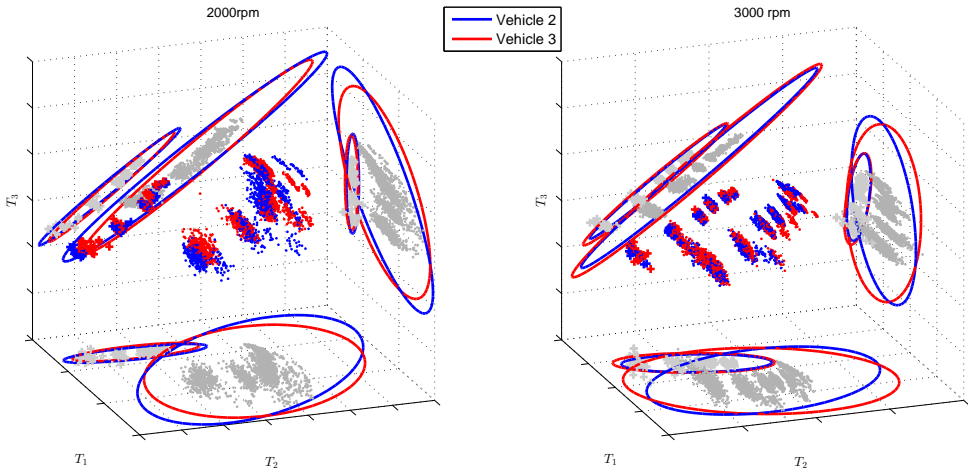


**Figure 6.6:** Estimated torque at crank count 19 ( $T_1$ ), 20 ( $T_2$ ) and 21 ( $T_3$ ). Values which belongs to misfires are marked as +. The ellipses around the projections on the different axes represent the requirements.

### 6.3 Torsional vibrations in the crankshaft

When a misfire occur, it results in an instantaneous reduction in the provided engine torque. This disturbance causes a torsional vibration in the crankshaft and driveline which create an oscillation in the measured signal that in the worst case inflicts false alarms, see Figure 6.7. Oscillations in the test quantity were also observed in [12] and pointed out as the primary cause of false alarms.

The cause of these false alarms are oscillations with large amplitude and short wavelength i.e., the system is under-damped and the measurements varies considerably and fast. At higher speeds the oscillations are damped by the inertia of the rotating pistons, and thus the problem with oscillations are minor. To reduce the risk of false alarms due to oscillations following a misfire, a model-based approach to compensate this behavior is developed.

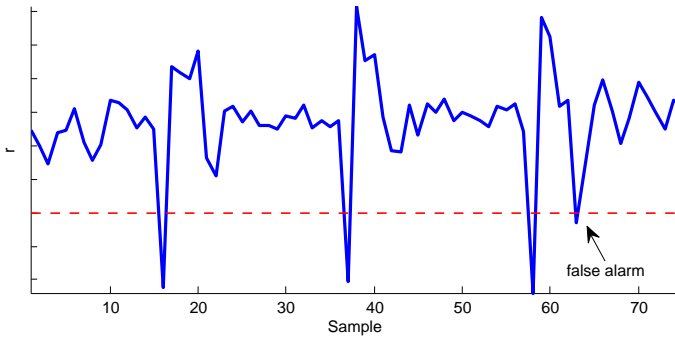


**Figure 6.7:** False alarm as a result of an oscillation in the test quantity after a real misfire.

#### 6.3.1 Model

The oscillations are not very distinct in the estimated torque if all samples are plotted. If instead the mean value of all samples in each combustion is used, the appearance of the oscillations become distinct, see Figure 6.8, with a similar appearance as the test quantity in Figure 6.7.

In [17] it is suggested to compensate for the oscillating behaviour by storing wave forms in the algorithm to filter out the effect of torsional vibrations. Here the oscillation has a behavior similar to the one of an exponentially damped sinusoid and thus can be described by the equation

$$T_{mean}(x) = Ae^{-\lambda x} \cos(\omega x + \Phi) \quad (6.4)$$

where  $A$  is the amplitude,  $\lambda$  the damping constant,  $\omega$  angular frequency and  $\Phi$  the phase angle.

The oscillations vary both depending on speed and load and as shown in Figure 6.9, where the model is fitted to data, also differ depending on which cylinder

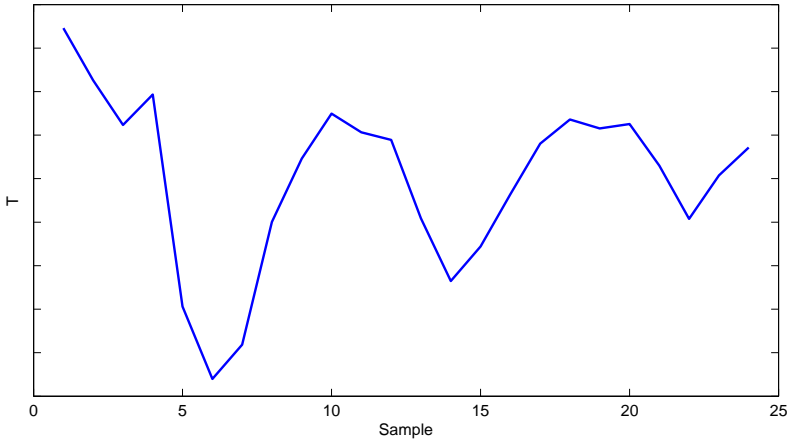


**Figure 6.8:** Mean estimated torque for each combustion after a misfire. An oscillation with similar behaviour as an exponentially damped sinusoid can be observed.

the misfire occur in. To manage this, the oscillations are modelled depending on speed, load and cylinder.

### 6.3.2 Compensation

In the estimated torque signal it is primary the first undershoot, which can be observed in Figure 6.8 and Figure 6.9 between sample 4 and 8, that is problematic and causes false alarms. The low torque values that follow as a consequence of the undershoot, causes an increased risk of misclassification. Even though both operating points based on speed and load are used the oscillation form vary within the operating points. In [17], it is pointed out that different gears result in different wave forms and thus different models might be needed. To avoid increasing the risk of false alarms if the model has a slightly offset to measured data, no compensations for the overshoots are made and the compensation is limited to removing the first undershoot. This is made by

$$t_k = t_k - f(k, \alpha), \quad (6.5)$$

where  $t_k = (T_1, T_2, T_3, T_4, T_5, T_6)$  is the normalized estimated torque with removed mean for each combustion  $k$  and  $f(k, \alpha)$  is the model described by (6.4) with the known parameters  $\alpha = (A, \lambda, \omega, \Phi)$ .

The parameterization of the model is done automatically using a Matlab curve-fitting function, `lsqcurvefit`, which solves the problem in least-squares sense on training data for each operating point. An example of resulting torque after the compensation is displayed in Figure 6.10. The compensation removes the

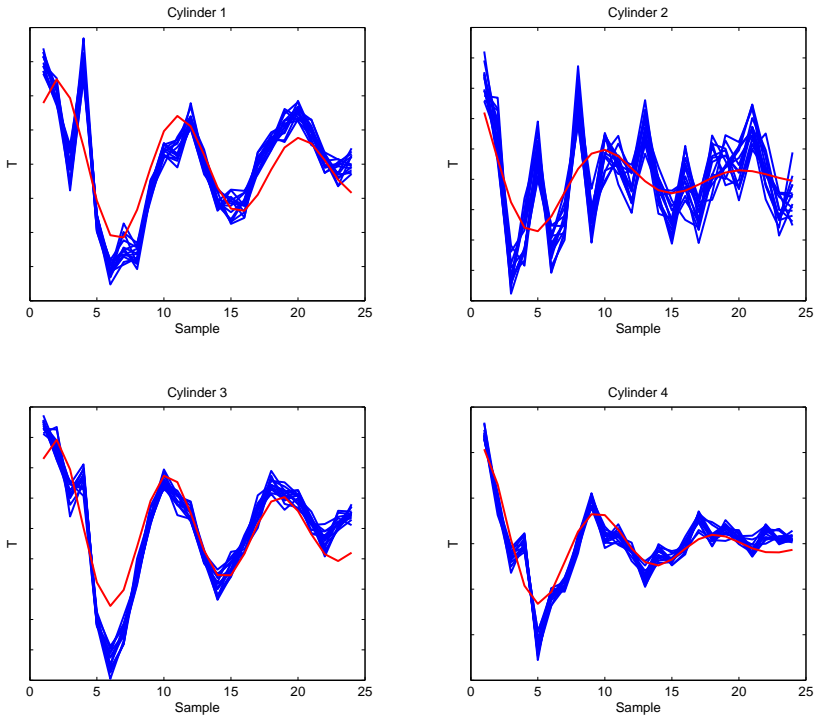


**Figure 6.9:** Mean estimated torque following several misfires in each cylinder separate. The red curve is the fitted model according to 6.4

problematic first wave trough which is the cause of false alarms. The remaining variations in the signal are within the normal differences between combustions and can be handled in the classification.

Further evaluation is carried out in Section 7.3 where this compensation is implemented in the detection algorithm and used on validation data. Since the oscillations vary both depending on speed, load and also differ depending on in which cylinder the misfire occur. Data also needs to be categorized based on load when training the algorithm, Step 2 in Section 4.5. As the problem with oscillations is minor at higher engine speeds the compensation is limited to engine speeds below 2500rpm. Furthermore no observations of oscillations causing false alarms have been made during cold start, thus the compensation for torsional vibrations is limited to normal driving conditions. Eight loads, four speeds and the four cylinders result in a total 128 operating points where the model needs to be parameterized in the algorithm. The model has 4 parameters that needs to be stored in each operating point which result in totaly 512 parameters.

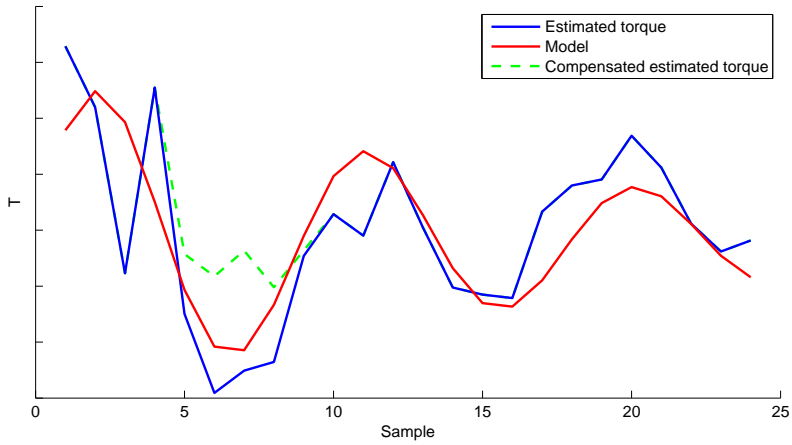


**Figure 6.10:** Mean estimated torque after a misfire with and without compensation for oscillations. The red curve is the fitted model according to (6.4)



# 7

---

## Evaluation

The evaluation in this chapter is carried out in three steps. First, the results when the misfire detection algorithm is trained without compensation for vehicle to vehicle variation or oscillations after a misfire are presented. Then, the performance of the algorithm with compensation for vehicle to vehicle variation is evaluated and finally also the compensation for torsional vibrations in the crankshaft after a misfire is introduced. All the results are compared and discussed in terms of the number of false alarms and missed detections but also using the Kullback-Leibler divergence in correlation to Volvo KPI.

### 7.1 Training and validation data

The training of the misfire detection algorithm is done according to the description in Section 4.5. All weights and thresholds are automatically optimized with SVM and the parameters in the oscillation model are automatically obtained with the `Matlab` curve-fitting function, `lsqcurvefit`. The algorithm is trained with data set 7 from Table 2.1 which contain steady state measurements from vehicle 2 to cover all engine modes including cold starts.

The training data include 540083 combustions of which 8676 contain injected misfires. For validation data sets 1-6 are used. The compensation for vehicle to vehicle variations require that steady state measurements are available for accurately calibration and thus only data set 5 and 6 are considered in the evaluation.

## 7.2 Evaluation of misfire detection algorithm

In Table 7.1, the results from the misfire detection algorithm are presented in terms of number of false alarms and missed detections.

Important to note is that the threshold is set in the middle of the margin between the distributions according to SVM and not according to the requirements in Section 5.2. Here the probability of false alarm is acceptable only in data set 5. Potentially the requirement could be met in more data sets if the threshold instead was selected according to the requirements.

The large amount of false alarms in data set 6 are caused by differences between the vehicles in the validation data and the training data, the vehicle to vehicle compensation is introduced and evaluated in Section 7.3. In data set 2, several of the false alarms originates from oscillations in the test quantity as a result of torsional vibrations after a real misfire, the compensation for torsional vibrations in the crankshaft are implemented and evaluated in Section 7.4.

Disregarding data set 6, cylinder 2 and 4 are overrepresented with 29 of the total 38 false alarms. This is compliant with the conclusion in Section 6.1.2 that these cylinders are especially problematic for misfire detection. Furthermore, all false alarms occur during normal driving and mainly take place at lower speeds and loads. In Figure 7.1 the false alarms and missed detections from data set 1, 2, 3 and 4 are plotted to show the main problematic operating conditions.

The separation between  $p_{mf}$  and  $p_{nf}$  in the test quantises are quantified with the Kullback-Leibler divergence for each speed operating point and cylinder and the results are shown in Tables 7.2, 7.3, 7.4, and 7.5. In the tables, the ratio between the standard deviation of misfire data and fault-free data are also shown to enable correlation to the requirements. Together with Figure 5.2, the tables can be used to draw conclusions if the distributions are separated enough to fulfill the requirements.

In the computation of the Kullback-Leibler divergence, data set 1, 2, and 3 are lumped together in order to obtain distributions with more data points at higher speeds. However, still only a few misfire data points are available at higher

Data set	Vehicle	Fault-free	Misfire	FA	Miss
1	1	67177	3617	6	1
2	1	65968	3085	20	8
3	1	71164	3477	6	2
4	2	30485	1510	5	0
5	3	562822	10380	1	3
6	4	90565	1667	8651	9

**Table 7.1:** Evaluation of the misfire detection algorithm.

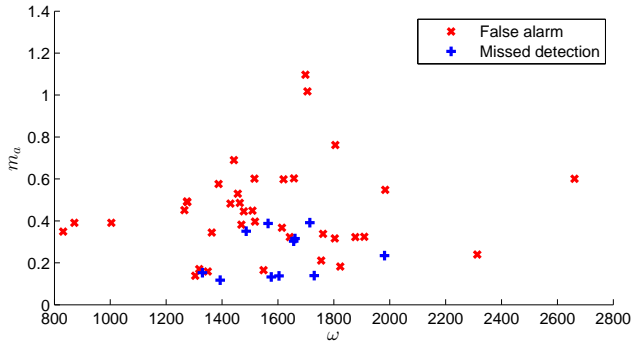


**Figure 7.1:** Plot showing at which speeds and loads false alarms and missed detections occur in data set 1, 2 and 3.

speeds which could explain the high ratios between the standard deviations in Table 7.2 and also in 7.3. Therefore the results at higher speeds in data set 1-4, which indicate that the detectability is low, are considered as uncertain. The absence of false alarms and missed detections at higher speeds also suggest that the separation is sufficient.

Overall, the Kullback-Leibler divergence is lower compared to the computed values in the misfire detectability analysis in Section 6.1.2. This can be explained by the reduction from six dimensions to one when creating the test quantity. The values in all data sets indicates worst performance in cylinder 2 and 4 around 1500-2000rpm, which confirm with the observed false alarms in Figure 7.1.

Cylinder	Speed [rpm]			
	1000	1500	2000	2500
1	27.91	19.14	21.10	32.10
$\sigma_{mf}/\sigma_{nf}$	0.38	0.37	0.82	0.95
2	21.05	12.55	13.71	15.46
$\sigma_{mf}/\sigma_{nf}$	0.23	0.32	0.59	0.53
3	21.67	17.23	21.70	29.67
$\sigma_{mf}/\sigma_{nf}$	0.16	0.36	0.90	1.96
4	20.18	15.08	18.20	20.98
$\sigma_{mf}/\sigma_{nf}$	0.74	0.50	0.88	1.39

**Table 7.2:** Kullback-Leibler divergence and standard deviation ratio for the test quantity obtained from data set 1,2 and 3.

Cylinder	Speed	[rpm]					
	1000	1500	2000	2500	3000	3500	4000
1	39.21	33.00	31.34	30.51	54.48	49.21	37.85
$\sigma_{mf}/\sigma_{nf}$	0.30	0.43	0.60	2.08	3.19	3.74	5.64
2	27.94	19.98	16.43	15.94	25.72	28.59	21.61
$\sigma_{mf}/\sigma_{nf}$	0.10	0.24	0.26	0.53	0.85	1.45	2.71
3	30.92	41.77	46.62	27.93	41.59	33.79	34.71
$\sigma_{mf}/\sigma_{nf}$	0.16	0.48	0.74	1.46	2.03	1.94	2.66
4	23.11	28.68	22.89	14.91	27.91	28.93	21.00
$\sigma_{mf}/\sigma_{nf}$	0.50	0.38	0.59	1.00	1.26	1.61	1.44

**Table 7.3:** Kullback-Leibler divergence and standard deviation ratio for the test quantity obtained from data set 4.

Cylinder	Speed	[rpm]							
	1000	1500	2000	2500	3000	3500	4000	4500	5000
1	25.43	43.12	24.75	52.19	83.11	52.33	75.49	110.40	111.68
$\sigma_{mf}/\sigma_{nf}$	0.52	0.25	0.23	0.45	0.91	0.72	0.62	0.71	0.29
2	20.60	46.11	27.87	26.20	19.49	27.36	51.67	59.44	55.74
$\sigma_{mf}/\sigma_{nf}$	0.22	0.20	0.15	0.30	0.44	0.43	0.55	0.77	0.33
3	21.02	95.62	35.30	38.99	27.38	22.03	35.36	82.21	58.45
$\sigma_{mf}/\sigma_{nf}$	0.17	0.28	0.22	0.54	0.72	0.36	0.29	1.13	0.36
4	33.43	42.07	30.97	24.47	40.32	41.81	46.89	30.13	61.55
$\sigma_{mf}/\sigma_{nf}$	0.52	0.16	0.27	0.31	0.37	0.49	0.24	0.30	0.36

**Table 7.4:** Kullback-Leibler divergence and standard deviation ratio for the test quantity obtained from data set 5.

Cylinder	Speed	[rpm]	
	2000	3500	5000
1	32.27	40.18	4.87
$\sigma_{mf}/\sigma_{nf}$	0.19	0.95	1.24
2	25.91	23.30	37.30
$\sigma_{mf}/\sigma_{nf}$	0.05	0.36	0.24
3	61.30	22.68	16.18
$\sigma_{mf}/\sigma_{nf}$	0.36	0.51	0.44
4	34.82	29.03	4.04
$\sigma_{mf}/\sigma_{nf}$	0.10	1.65	1.07

**Table 7.5:** Kullback-Leibler divergence and standard deviation ratio for the test quantity obtained from data set 6.

## 7.3 Compensation for vehicle to vehicle variations

For an accurate vehicle to vehicle compensation, steady state measurements are required in the calibration. The parameter  $b_\theta$  is found with the method described in Section 6.2.1 and implemented according to (6.1) in the angular velocity equation in the algorithm.

As steady state measurements are required, the compensation is applied on data set 5 and 6 only. The calibration to find  $b_\theta$  is done in both vehicles with data collected at 5000 rpm and load 0.8. The results after the compensation are presented in Table 7.6 and the corresponding Kullback-Leibler divergences are presented in Table 7.7 and 7.8.

The compensation give a performance gain for both data sets in terms of a reduced number of missed detections and a large reduction in false alarms in data set 6. When comparing the computed Kullback-Leibler divergence before and after the compensation, even if a few operating points have a slightly reduced values, the pervading conclusion is an performance gain also in terms of separation. All the operating points lies above the requirements and thus indicate that the distributions have the required separation. In Figure 7.2 and Figure 7.3 histograms of the test quantity for data set 6 with and without the compensation are displayed. After the compensation, the distributions obtain more distinct peaks and larger margin to the threshold which means misclassification can be avoided.

Data set	Vehicle	Fault-free	Misfire	FA	Miss
5	3	562822	10380	2	0
6	4	90565	1667	1	0

**Table 7.6:** Evaluation of the misfire detection algorithm after compensation of vehicle variation.

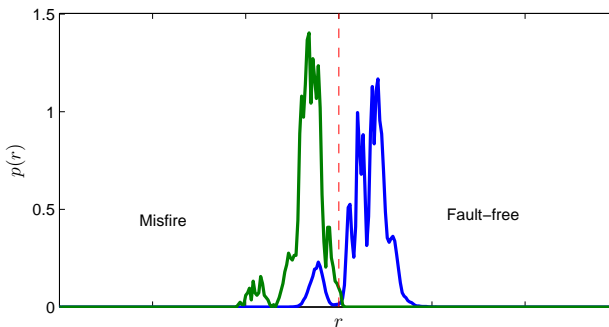


**Figure 7.2:** Histogram of the test quantity  $r$  given data set 6 without compensation for vehicle to vehicle variation. The separating line represent the threshold parameterized using SVM.

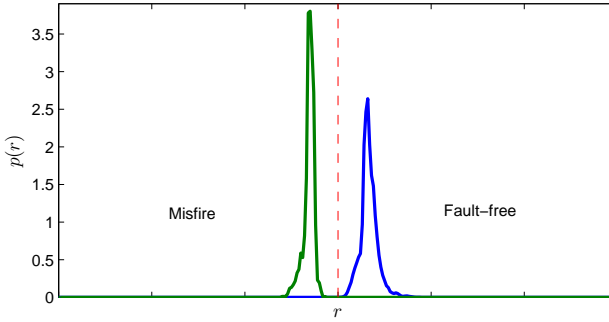


**Figure 7.3:** Histogram of the test quantity  $r$  given data set 6 with compensation for vehicle to vehicle variation. The separating line represent the threshold parameterized using SVM.

Cylinder	Speed [rpm]								
	1000	1500	2000	2500	3000	3500	4000	4500	5000
1	25.67	48.48	23.03	62.12	83.12	72.13	96.48	114.18	124.90
$\sigma_{mf}/\sigma_{nf}$	0.54	0.20	0.23	0.42	0.91	0.89	0.70	0.66	0.28
2	21.56	47.93	26.48	26.26	28.01	41.58	57.24	55.75	70.94
$\sigma_{mf}/\sigma_{nf}$	0.21	0.18	0.16	0.30	0.29	0.55	0.63	0.94	0.43
3	22.03	93.20	29.88	47.48	47.82	38.85	52.54	57.18	69.65
$\sigma_{mf}/\sigma_{nf}$	0.15	0.35	0.26	0.50	0.54	0.34	0.26	1.55	0.27
4	32.75	45.40	34.93	30.00	41.16	45.84	57.34	40.00	55.81
$\sigma_{mf}/\sigma_{nf}$	0.52	0.15	0.23	0.26	0.35	0.65	0.31	0.42	0.41

**Table 7.7:** Kullback-Leibler divergence and standard deviation ratio for the test quantity obtained from data set 5 after compensation for vehicle variation.

Cylinder	Speed [rpm]		
	2000	3500	5000
1	29.92	66.71	38.56
$\sigma_{mf}/\sigma_{nf}$	0.17	0.31	1.55
2	26.62	45.98	35.40
$\sigma_{mf}/\sigma_{nf}$	0.04	0.50	1.43
3	61.18	58.23	68.69
$\sigma_{mf}/\sigma_{nf}$	0.36	0.26	0.98
4	37.43	32.75	33.72
$\sigma_{mf}/\sigma_{nf}$	0.11	0.11	0.86

**Table 7.8:** Kullback-Leibler divergence and standard deviation ratio for the test quantity obtained from data set 6 after compensation for vehicle variation.

## 7.4 Compensation for torsional vibrations

The compensation for torsional vibrations following a misfire are included in the misfire detection algorithm and applied on data set 1-6. The compensation with the parameterized model described by (6.4) is activated when a misfire is detected and is limited to removing the first undershoot.

The calibration for vehicle to vehicle variations described in Section 7.3 is still applied on data set 5 and 6. The result in the number of false alarms and missed detections is presented in Table 7.9 and the computed Kullback-Leibler divergences are presented in Tables 7.10, 7.11, 7.12 and 7.13.

In data sets 1-4 the number of false alarms are reduced which indicates that the compensation serves its purpose. There are still a few false alarms that comes as a result of oscillations when the compensation was not sufficient, or the measured data deviates from the modeled behaviour. In the cases where the measured data deviates within an operating point the used static model is not valid and instead an increased risk for missed detection is introduced.

Some of the remaining missed detections in data sets 1-3 could be explained by that the compensation for vehicle to vehicle variations is not applied. The com-

Data set	Vehicle	Fault-free	Misfire	FA	Miss
1	1	67177	3617	5	1
2	1	65968	3085	9	8
3	1	71164	3477	5	2
4	2	30485	1510	3	0
5	3	562822	10380	2	0
6	4	90565	1667	1	0

**Table 7.9:** Evaluation of the misfire detection algorithm.

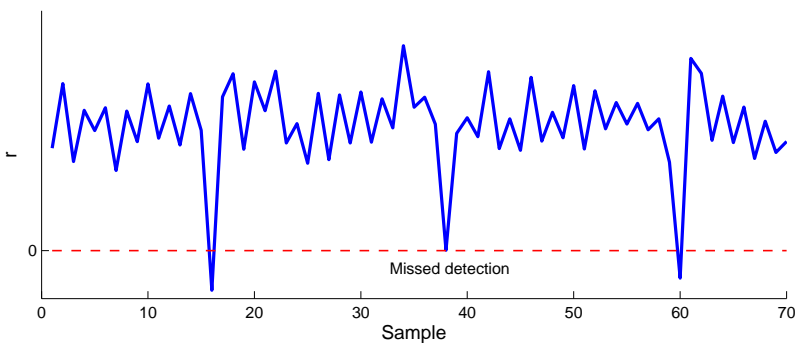


**Figure 7.4:** Test quantity from data set 2 computed from measurements around 1600 rpm. A missed detection occur around sample 38.

compensation for vehicle to vehicle variations potentially accomplish a greater similarity between the training data and validation data. Thereby missed detections such as in Figure 7.4, where the threshold is not optimally set relative to the validation data could possibly be avoided.

Remaining false alarms are caused by several different reasons. One observed source of error that cause a few false alarms is a fast reduction in engine speed. The reduction could be caused by gear shifting or heavy breaking and further investigations are required to avoid these false alarms.

The Kullback-Leibler divergence and the standard deviation ratio indicate that the performance has been slightly increased in most of the operating points for the previously problematic cylinders 2 and 4, while a slight reduction in the performance is observed in cylinder 1 and 3. This can be explained by that some data points of  $p_{nf}$  are moved away from the expected value such that the distribution tail directed away from  $p_{mf}$  becomes larger. As the distributions are approximated as Gaussian, this leads to a higher variance for the fault-free data and thus lower Kullback-Leibler divergence, see (5.2). This is visualised in Figure 7.5 and Figure 7.6 where histograms of the test quantity before and after the compensation for oscillations are plotted, where the dashed line is the fault-free distribution before the compensation. Figure 7.6 shows a cylinder and operating point where the Kullback-Leibler divergence indicates a reduced performance and in Figure 7.5 the Kullback-Leibler divergence indicates improved performance.

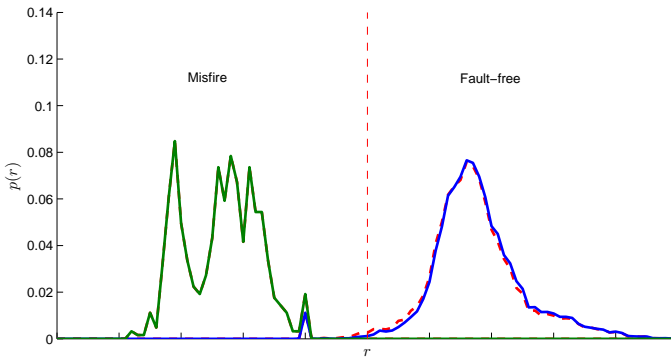


**Figure 7.5:** Histogram of the test quantity  $r$  before and after compensation for oscillations. The dotted line represent the fault-free distribution before the compensation, here the compensation increase the Kullback-Leibler divergence.

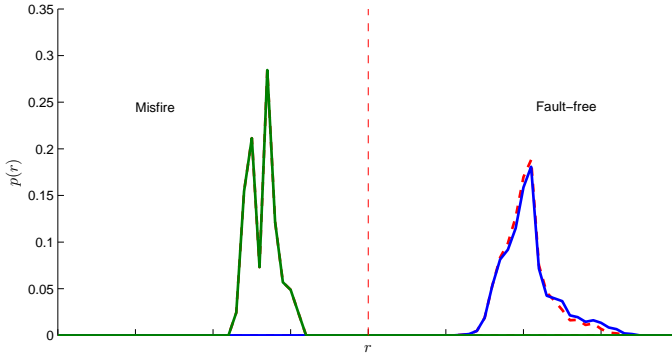


**Figure 7.6:** Histogram of the test quantity  $r$  before and after compensation for oscillations. The dotted line represent the fault-free distribution before the compensation, here the compensation reduce the Kullback-Leibler divergence.

Cylinder	Speed [rpm]			
	1000	1500	2000	2500
1	27.74	19.28	20.96	31.61
$\sigma_{mf}/\sigma_{nf}$	0.38	0.37	0.79	0.92
2	21.02	12.98	14.83	17.06
$\sigma_{mf}/\sigma_{nf}$	0.23	0.32	0.62	0.57
3	21.67	16.85	20.10	27.70
$\sigma_{mf}/\sigma_{nf}$	0.16	0.34	0.81	1.79
4	19.88	15.17	18.04	19.38
$\sigma_{mf}/\sigma_{nf}$	0.72	0.49	0.84	1.26

**Table 7.10:** Kullback-Leibler divergence and standard deviation ratio for the test quantity obtained from data set 1,2 and 3 with compensation for oscillations in the test quantity.

Cylinder	Speed [rpm]						
	1000	1500	2000	2500	3000	3500	4000
1	39.33	33.85	32.56	29.96	54.48	49.21	37.85
$\sigma_{mf}/\sigma_{nf}$	0.30	0.43	0.60	2.08	3.19	3.74	5.64
2	28.22	20.75	17.66	16.98	25.72	28.59	21.61
$\sigma_{mf}/\sigma_{nf}$	0.10	0.24	0.26	0.53	0.85	1.45	2.71
3	31.03	43.24	47.45	28.05	41.59	33.79	34.71
$\sigma_{mf}/\sigma_{nf}$	0.16	0.48	0.74	1.46	2.03	1.94	2.66
4	22.98	29.20	23.06	15.06	28.03	28.93	21.00
$\sigma_{mf}/\sigma_{nf}$	0.50	0.38	0.59	1.00	1.26	1.61	1.44

**Table 7.11:** Kullback-Leibler divergence and standard deviation ratio for the test quantity obtained from data set 4 with compensation for oscillations in the test quantity.

Cylinder	Speed [rpm]		2000	2500	3000	3500	4000	4500	5000
	1000	1500							
1	25.50	43.31	19.64	39.36	83.12	72.13	96.48	114.18	124.90
$\sigma_{mf}/\sigma_{nf}$	0.53	0.17	0.19	0.26	0.91	0.89	0.70	0.66	0.28
2	22.21	51.88	26.90	26.90	28.01	41.58	57.24	55.75	70.94
$\sigma_{mf}/\sigma_{nf}$	0.22	0.19	0.16	0.30	0.29	0.55	0.63	0.94	0.43
3	21.92	78.94	24.69	32.64	47.82	38.85	52.54	57.18	69.65
$\sigma_{mf}/\sigma_{nf}$	0.15	0.29	0.21	0.33	0.54	0.34	0.26	1.55	0.27
4	28.07	43.70	28.49	23.86	41.16	45.84	57.34	40.00	55.81
$\sigma_{mf}/\sigma_{nf}$	0.44	0.14	0.18	0.20	0.35	0.65	0.31	0.42	0.41

**Table 7.12:** Kullback-Leibler divergence and standard deviation ratio for the test quantity obtained from data set 5 after compensation for vehicle variation and compensation for oscillations in the test quantity.

Cylinder	Speed [rpm]		
	2000	3500	5000
1	24.60	66.71	38.56
$\sigma_{mf}/\sigma_{nf}$	0.14	0.31	1.55
2	28.26	45.98	35.40
$\sigma_{mf}/\sigma_{nf}$	0.04	0.50	1.43
3	47.68	58.23	68.69
$\sigma_{mf}/\sigma_{nf}$	0.27	0.26	0.98
4	32.28	32.75	33.72
$\sigma_{mf}/\sigma_{nf}$	0.09	0.11	0.86

**Table 7.13:** Kullback-Leibler divergence and standard deviation ratio for the test quantity obtained from data set 6 after compensation for vehicle variation compensation for oscillations in the test quantity.

## 7.5 Summary and discussion

The evaluation shows that the original misfire detection algorithm give varying results. The largest error was observed in data set 6 due to vehicle to vehicle variations which indicates that calibration of the algorithm is essential to obtain a robust result. In data sets 1-4, several false alarms caused by torsional vibrations following misfires are observed and compensation is necessary to improve the performance. In the evaluation, the two suggested and implemented compensations for these problems, improve the performance in terms of number of false alarms and missed detections without significantly increasing the complexity.

The compensation for vehicle to vehicle variations shows good results on the steady state measurements with reduced number of false alarms and missed detections but also an increased separation according to the Kullback-Leibler divergence. After the compensation, the correlated requirements in Volvo KPI are met in all operating points. However, no validation against real measurements on the road are done, as in the suggested method the correction factor  $b_\theta$  need to be found with steady state measurements from both the training data and validation data. The dependency of steady state measurements can be avoided by using the method in [4], where systematic errors are found by shutting of the fuel supply to the engine, to obtain a smooth deceleration from high speed without interference from cylinder compressions.

In the current method the mean estimated torque from one stationary operating point is used to find  $b_\theta$ . For a more robust result, the average  $b_\theta$  from several operating points could be used. This would possible reduce the dependency on similarity of calibration data but increase the amount of stored calibration data in the algorithm.

The compensation for the oscillations in the signal after a misfire is shown to remove some of the false alarms, but in certain cases fail to compensate for the problematic behaviour. When the model fail to describe the oscillatory behaviour it may instead increase the risk for missed detection. No measurements with multiple misfires are available in the validation, so the potential increased risk for missed detection can not be evaluated. An increased risk for missed detection could originate both from the oscillation peaks, overcompensation or model offset. Additional investigation and development of the oscillation compensation would therefore be interesting and probably further improve the misfire detection algorithm.



# 8

---

## Conclusions and future work

In this final chapter a short summary of the thesis is given together with suggestions on future work to improve the developed misfire detection algorithm.

### 8.1 Conclusions

A model-based misfire detection algorithm suitable for on-board diagnostics is presented and evaluated against real measurements. As in [12], a simplified engine model, with low required computational power, is suggested to estimate torque from the flywheel angular velocity signal. The estimated torque has the advantage that at similar operating speeds and loads it obtains resembling values and different combustions can be compared. The signal is processed such that no dependencies on load remain and thus the estimated torque is categorized in operating points based on cylinder, speed and if cold start occur.

A test quantity for classification is then created by weighing all samples of the estimated torque related to each combustion. The weights as well as the threshold are optimized using SVM to obtain maximal separation between fault-free data and misfire data. To compensate for vehicle to vehicle variations due to manufacturing imperfections of the flywheel, a simple method is proposed with only one parameter per teeth interval to be calibrated. The compensation enables accurate misfire detection for various vehicles with the same training data. The method is validated on steady state measurements with successful results, both in a reduced number of false alarms and missed detections as well as an increased Kullback-Leibler divergence.

By modeling oscillations following a misfire as an exponentially damped sinusoid and filter the signal with the model after a misfire, the number of false alarms are reduced.

The Kullback-Leibler divergence correlated to Volvo KPI is used to compare and evaluate the detectability performance. In the analysis, significant differences between the cylinders are observed in the four cylinder vehicle and therefore no overall advantage compared to the six cylinder is obtained. The differences between cylinders are confirmed in the validation of algorithm as the problematic cylinders are overrepresented when the false alarms are investigated.

Overall the misfire detection algorithm perform well and give few false alarms and missed detections. This indicates that the used simplified engine crankshaft model and the pre-processing of the estimated torque enhances the effects of a misfires enough to be detected. However, the result in several data sets do not meet the requirements in Volvo KPI. The requirements potentially could be met if the threshold was set according to the requirements instead of in the middle of the margin according to SVM.

The evaluation with the Kullback-Leibler divergence also give ambiguous results, and the worst performing cylinders at certain speeds do not achieve the requirements in Volvo KPI. However this is in data sets where no compensation for vehicle to vehicle variations are used, since no steady state measurements are available, and such compensation would probably increase the Kullback-Leibler divergence. Prior to any possible implementation, the calibration of vehicle to vehicle variations thus needs to be further evaluated with more data from vehicle on road for better validation. Regarding the compensation for torsional vibration, the compensation is not robust and further investigation need to be carried out to fully compensate for the complex oscillating behaviour.

## 8.2 Future work

As the performance of the algorithm with fault-compensation all depend on the training data used for parameterization, an analysis of which kind of measurements that give best performance would be interesting. The steady state measurements from a chassis dynamometer used for the parameterization in this work exclude certain behaviours that is present in real driving scenarios.

For the same reason the developed misfire detection algorithm need additional testing with measurements from real driving scenarios on the road, with varying environmental conditions for a more extensive evaluation. Furthermore multiple misfires injected shortly after each other should be considered especially to investigate if the compensation for oscillations introduce a major risk for missed detections.

A limitation in the presented misfire detection algorithm is that the compensation for vehicle to vehicle variations requires steady state measurements to estimate  $b_\theta$  and needs to be calibrated prior to the use of the algorithm. A method that enable estimation of  $b_\theta$  on-line such as the one presented in [4] could remove the limitation in the compensation for vehicle to vehicle variations. Such method also would reduce the impact of wear out errors since calibration may be ongoing.

Certain false alarms were observed due to a fast reduced engine speed. An investigation to isolate the cause and establish a method on how to manage the speed reduction, could remove additional false alarms and thereby improve the algorithm performance.

Another possible improvement of the algorithm performance could be obtained by different choices of operating points. The false alarms and missed detections registered in the evaluation in the existing algorithm all occur at similar speed and load. Additional operating points in problematic intervals could be used to increase separation of data in each operating point.

A model that describe the behaviour of the inertial torque and thus could expose the torque produced during the combustion would increase the detectability of misfires. Such model would also possibly solve the problem with varying performance in different cylinders and also reduce the number of modes as all cylinders could be considered together. However, such new model must retain low complexity in order to enable on-line detection.



---

## Bibliography

- [1] Malfunction and diagnostic system requirements–2004 and subsequent model-year passenger cars, light-duty trucks, and medium-duty vehicles and engines. *Section 1968.2, Title 13, California Code of Regulations*. Cited on pages 1 and 22.
- [2] Christopher M. Bishop. *Pattern Recognition and Machine Learning (Information Science and Statistics)*. Springer-Verlag New York, Inc., Secaucus, NJ, USA, 2006. ISBN 0387310738. Cited on pages 20 and 22.
- [3] George Casella and Roger L. Berger. *Statistical Inference*. Duxbury resource Center, Pacific Grove, CA, second edition, 2001. Cited on page 22.
- [4] J.M. Dossdall and J.V. James. Correction of systematic position-sensing errors in internal combustion engines, June 2 1992. US Patent 5,117,681. Cited on pages 51 and 54.
- [5] Daniel Eriksson. Diagnosability analysis and FDI system design for uncertain systems. Technical report, 2013. LiU-TEK-LIC-2013:18, Thesis No. 1584. Cited on page 31.
- [6] Lars Eriksson and Ingemar Andersson. An Analytic Model for Cylinder Pressure in a Four Stroke SI Engine. *SAE Transactions, Journal of Engines, 2002-01-0371*, 111(3), September 2003. Cited on page 4.
- [7] Jürgen Förster, Andrea Lohmann, Manfred Mezger, and Klaus Ries-Müller. [advanced engine misfire detection for si-engines. Cited on pages 1, 4, and 8.
- [8] Erik Frisk and Mattias Nyberg. *Model Based Diagnosis of Technical Processes*. Vehicular System, ISY Linköping Institute of Technology, 2013. Cited on page 3.
- [9] M.A Hearst, S.T. Dumais, E. Osman, J. Platt, and B. Scholkopf. Support vector machines. *Intelligent Systems and their Applications, IEEE*, 13(4): 18–28, Jul 1998. ISSN 1094-7167. doi: 10.1109/5254.708428. Cited on page 20.

- [10] John R. Hershey and Peder A. Olsen. Approximating the kullback leibler divergence between gaussian mixture models. *ICASSP*, 4(1):317–320, 2007. Cited on page 21.
- [11] Kazumasa Iida, Katsuo Akishino, and Kazuo Kido. [imep estimation from instantaneous crankshaft torque variation. Cited on pages 11, 13, and 14.
- [12] Daniel Jung, Lars Eriksson, Erik Frisk, and Mattias Krysanter. Development of misfire detection algorithm using quantitative FDI performance analysis. *Control Engineering Practice*, 34(0):49 – 60, 2015. ISSN 0967-0661. Cited on pages 2, 3, 4, 5, 9, 10, 11, 14, 17, 18, 22, 27, 32, 36, and 53.
- [13] U. Kiencke. Engine misfire detection. *Control Engineering Practice*, 7(2): 203–208, 1999. Cited on pages 2, 4, 9, and 13.
- [14] Rudolf Kulhavý. A Kullback-Leibler Distance Approach to System Identification. *Annual Reviews in Control*, 20:119–130, 1996. Cited on page 5.
- [15] Ken-je Langn, Lela Liu, Alec L. Lang, and Louis Yizhang Liu. Multi-Purpose Flywheel (MPF) and Misfire Detection. *SAE Technical Paper 2005-01-1141*, 2005. Cited on page 32.
- [16] J Mohammadpour, M Franchek, and K Grigoriadis. A survey on diagnostic methods for automative engines. *International Journal of Engine Research*, 13(1):41–64, 2012. Cited on page 4.
- [17] Fabrizio Ponti and Luca Solieri. Analysis of the Interactions Between Indicated and Reciprocating Torque for the Development of a Torsional Behavior Model of the Powertrain. *Journal of Engineering for Gas Turbines and Power*, 130(1):119–130, 1996. Cited on pages 11, 14, 36, and 37.
- [18] William B. Ribbens and Giorgio Rizzoni. Onboard Diagnosis of Engine Misfires. *SAE Technical Paper 901768*, 1990. Cited on pages 1, 4, and 8.
- [19] E. Weißenborn, T. Bossmeyer, and T. Bertram. Adaptation of a zero-dimensional cylinder pressure model for diesel engines using the crankshaft rotational speed. *Meachanical Systems and Signal Processing*, 25(1):1887–1910, 1990. Cited on pages 11, 14, 32, and 35.



## Upphovsrätt

Detta dokument hålls tillgängligt på Internet — eller dess framtida ersättare — under 25 år från publiceringsdatum under förutsättning att inga extraordinära omständigheter uppstår.

Tillgång till dokumentet innebär tillstånd för var och en att läsa, ladda ner, skriva ut enstaka kopior för enskilt bruk och att använda det oförändrat för icke-kommersiell forskning och för undervisning. Överföring av upphovsrätten vid en senare tidpunkt kan inte upphäva detta tillstånd. All annan användning av dokumentet kräver upphovsmannens medgivande. För att garantera äktheten, säkerheten och tillgängligheten finns det lösningar av teknisk och administrativ art.

Upphovsmannens ideella rätt innefattar rätt att bli nämnd som upphovsman i den omfattning som god sed kräver vid användning av dokumentet på ovan beskrivna sätt samt skydd mot att dokumentet ändras eller presenteras i sådan form eller i sådant sammanhang som är kränkande för upphovsmannens litterära eller konstnärliga anseende eller egenart.

För ytterligare information om Linköping University Electronic Press se förlagets hemsida <http://www.ep.liu.se/>

## Copyright

The publishers will keep this document online on the Internet — or its possible replacement — for a period of 25 years from the date of publication barring exceptional circumstances.

The online availability of the document implies a permanent permission for anyone to read, to download, to print out single copies for his/her own use and to use it unchanged for any non-commercial research and educational purpose. Subsequent transfers of copyright cannot revoke this permission. All other uses of the document are conditional on the consent of the copyright owner. The publisher has taken technical and administrative measures to assure authenticity, security and accessibility.

According to intellectual property law the author has the right to be mentioned when his/her work is accessed as described above and to be protected against infringement.

For additional information about the Linköping University Electronic Press and its procedures for publication and for assurance of document integrity, please refer to its www home page: <http://www.ep.liu.se/>